Molecular Microbiology (2016) 00(00), 00–00 ■
doi:10.1111/mmi.13477
First published online 2016

The DnaA inhibitor SirA acts in the same pathway as Soj (ParA) to facilitate *oriC* segregation during *Bacillus subtilis* sporulation

Yi Duan, Jack D. Huey and Jennifer K. Herman*
Department of Biochemistry and Biophysics, Texas A&M University, College Station, TX, USA.

Summary

DNA replication and chromosome segregation must be carefully regulated to ensure reproductive success. During *Bacillus subtilis* sporulation, chromosome copy number is reduced to two, and cells divide asymmetrically to produce the future spore (forespore) compartment. For successful sporulation, *oriC* must be captured in the forespore. New rounds of DNA replication are prevented in part by SirA, a protein that utilizes residues in its N-terminus to directly target Domain I of the bacterial initiator, DnaA. Using a quantitative forespore chromosome organization assay, we show that SirA also acts in the same pathway as another DnaA regulator, Soj, to promote *oriC* capture in the forespore. By analyzing loss-of-function variants of both SirA and DnaA, we observe that SirA's ability to inhibit DNA replication can be genetically separated from its role in *oriC* capture. In addition, we identify substitutions near the C-terminus of SirA and in DnaA Domain III that enhance interaction between the two proteins. One such variant, $SirA_{P141T}$, remained functional in regard to inhibiting replication, but was unable to support *oriC* capture. Collectively, our results support a model in which SirA targets DnaA Domain I to inhibit DNA replication, and DnaA Domain III to facilitate Soj-dependent *oriC* capture in the forespore.

Introduction

In all bacteria for which origin of replication (*oriC*) dynamics have been examined, newly synthesized replication origins are segregated toward a cell pole (or future cell pole in cells with multifork replication) shortly after DNA replication initiation (Lewis and Errington, 1997; Sharpe and Errington, 1998; Niki *et al.*, 2000; Lemon and Grossman, 2001; Viollier *et al.*, 2004; Wang *et al.*, 2014a). *oriC* segregation happens with high fidelity and is aided by chromosome condensing and partitioning complexes that include MukBEF, SMC, and ParABS (Reyes-Lamothe *et al.*, 2012; Hirano, 2016). The MukBEF and SMC complexes include condensin proteins that compact the chromosome lengthwise (Hirano, 2016), while ParA and ParB orthologs have been found to stabilize the partitioning of both low copy-number plasmids and bacterial chromosomes (Gerdes *et al.*, 2000).

In *B. subtilis*, ParA and ParB are most often referred to as Soj and Spo0J, respectively. Spo0J binds to *parS* sites and forms a centromere-like nucleoprotein complex favorable for *oriC* segregation (Sharpe and Errington, 1996; Lee and Grossman, 2006). Spo0J-*parS* complexes are also important for SMC enrichment around the *oriC*-proximal region of the chromosome (Gruber and Errington, 2009; Sullivan *et al.*, 2009) and cohesion of the chromosomal arms following their replication (Wang *et al.*, 2015). A *spo0J* mutant exhibits a slight increase in the frequency of anucleate cells (Ireton *et al.*, 1994) and is important for *oriC* segregation in the absence of a functional SMC complex (Wang *et al.*, 2014b). Soj, which is encoded in the same operon as Spo0J, is not required for chromosome segregation during vegetative growth (Lee and Grossman, 2006). Instead, Soj's described function is to regulate DNA replication by interacting directly with the bacterial DNA initiator protein DnaA (Murray and Errington, 2008; Scholefield *et al.*, 2012). During replication initiation, DnaA binds to and oligomerizes at *oriC*. Soj binds to DNA as an ATP-dependent dimer, and directly stimulates DnaA to activate DNA replication initiation (Leonard *et al.*, 2005). Following replication initiation, the monomeric form of Soj acts as an inhibitor of initiation by preventing DnaA oligomerization (Scholefield *et al.*, 2012). Spo0J promotes Soj's ATPase activity, and

Accepted 1 August, 2016. *For correspondence. E-mail jkherman@tamu.edu; Tel. 979-862-3165; Fax 979-845-9274.

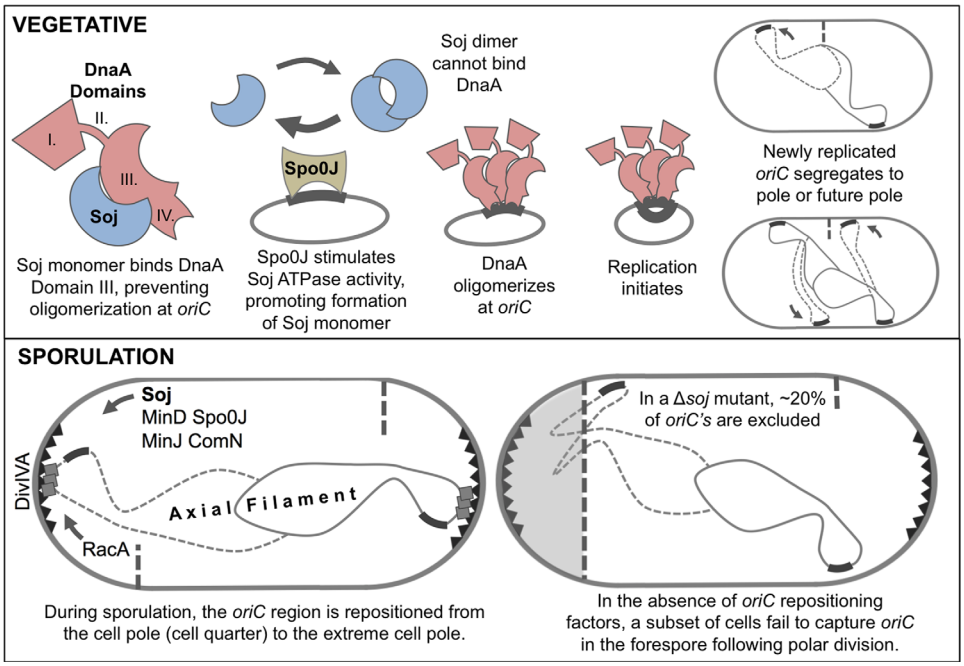

Fig. 1. (Top) Following DNA replication initiation, newly synthesized *oriC*s are repositioned at cell quarters and future cell quarters. Spo0J stimulates formation of Soj monomers, delaying new rounds of DNA replication initiation until an unknown cell cycle cue is received. (Bottom) During sporulation, *oriC* is repositioned from the cell quarter toward the extreme cell pole in a manner that depends on DivIVA (black triangles), RacA (grey squares), MinD, ComN, MinJ, Spo0J, and Soj. In the absence of factors important for *oriC* repositioning during sporulation, a subset of cells fail to capture *oriC* in the forespore compartment following polar septation.

thus also appears to function as a negative regulator of replication initiation in vivo (Fig. 1)(Scholefield *et al.*, 2011).

DNA replication and *oriC* dynamics are also highly regulated during bacterial development. For example, during sporulation, *B. subtilis* reduces its chromosome copy number to two and stretches the chromosomes along the cell length in an *oriC-ter-ter-oriC* arrangement called the axial filament (Bylund *et al.*, 1993; Piggot and Hilbert, 2004). The number of chromosomes in sporulating cells is regulated by nutrient status, a checkpoint protein called Sda (Burkholder *et al.*, 2001; Veening *et al.*, 2009), and by SirA, a protein expressed early in sporulation that directly targets DnaA activity (Wagner *et al.*, 2009). SirA ensures that new rounds of DNA replication are not initiated, thus preserving a diploidy state in the sporulating cell (Wagner *et al.*, 2009). Once the axial filament forms, septation occurs near one pole, initially capturing only a portion of one chromosome in the future spore (forespore) compartment (Wu and Errington, 2003; Sullivan *et al.*, 2009; Miller *et al.*, 2016). The remainder of the chromosome is eventually pumped into the forespore, but only if the chromosome's *oriC* region is captured on the forespore side of the polar septum (Becker and Pogliano, 2007). Therefore, the position of *oriC* at the time of polar septation is important for successful sporulation.

Several proteins have been implicated in *oriC* capture in the forespore (Ben-Yehuda *et al.*, 2003; Wu and Errington, 2003; Sullivan *et al.*, 2009). Spo0J condenses the *oriC*-proximal region into a centromere-like element favorable for chromosome segregation during both vegetative growth and sporulation (Sharpe and Errington, 1996). Another protein, RacA, contributes by tethering the *oriC*-proximal region to the distal cell pole via interactions with the polar organizing protein DivIVA (Fig. 1)(Ben-Yehuda *et al.*, 2003, 2005; Wu and Errington, 2003). The DnaA regulator Soj is also important, as a Δ*soj* mutant fails to capture *oriC* in ~20% of sporulating cells (Fig. 1)(Sullivan *et al.*, 2009). Genetic and cell biological data indicate that Soj's importance is amplified in the absence of a functional RacA tethering system, suggesting that these two systems contribute in independent ways (Wu and Errington, 2003); the precise role of Soj in *oriC* capture is unknown. Recently, Kloosterman *et al.* demonstrated that ComN, MinJ, and MinD, proteins that like RacA utilize DivIVA for localization (Bramkamp *et al.*, 2008; Patrick and Kearns, 2008; dos Santos *et al.*, 2012), also act in the same pathway as Soj to facilitate *oriC* capture (Fig. 1)(Kloosterman *et al.*, 2016). The authors propose that during sporulation, a complex of proteins that includes DivIVA, ComN, MinJ, and MinD relocalizes from the cell quarter to the extreme cell pole, and that this relocalization is important for Soj-dependent *oriC* capture (Kloosterman *et al.*, 2016).

Here we show that the sporulation protein SirA, which also regulates DnaA activity (Rahn-Lee *et al.*, 2009; Wagner *et al.*, 2009; Rahn-Lee *et al.*, 2011; Jameson *et al.*, 2014), is also required for high-fidelity *oriC* capture in the forespore. More specifically we show that SirA and Soj act in the same pathway to segregate *oriC* in 10% of sporulating cells. Residues in the N-terminus of SirA

interact directly with DnaA Domain I to inhibit replication (Jameson *et al*., 2014), and SirA inhibits new rounds of DNA replication initiation during sporulation (Wagner *et al*., 2009). Surprisingly, we found that SirA's ability to inhibit DNA replication is not required for its role in *oriC* capture, indicating that these functions are distinct and separable. Using SirA-DnaA gain of interaction screens, we identified additional residues near the C-terminus of SirA and in DnaA Domain III, which are also important for mediating interaction between the two proteins. Moreover, we isolated one C-terminal substitution in SirA, P141T, which inhibits DNA replication, yet is unable to support SirA-dependent *oriC* capture. These unexpected results suggest that SirA may target two distinct domains of DnaA: Domain I, to inhibit DNA replication, and Domain III to facilitate Soj-dependent *oriC* segregation.

Results

A ΔsirA *mutant has an* oriC *segregation defect during sporulation*

Soj interacts directly with DnaA Domain III (Murray and Errington, 2008; Scholefield *et al*., 2012) and is required for the high fidelity capture of *oriC* in the forespore compartment (Sullivan *et al*., 2009). SirA also interacts with DnaA (Wagner *et al*., 2009; Jameson *et al*., 2014) and a Δ*sirA* mutant is reported to have a defect in organization of the axial filament during sporulation (Wagner *et al*., 2009). Since Soj and SirA both regulate DnaA activity directly, we hypothesized that SirA and Soj might both act through a DnaA-dependent pathway to facilitate *oriC* segregation during sporulation. To test this idea, we determined the location of *oriC* in a Δ*sirA* mutant using a single cell chromosome organization assay that provides a readout of regions of DNA captured or "trapped" in the forespore compartment during sporulation (Sullivan *et al*., 2009). We found that 10% of cells in the Δ*sirA* mutant population failed to trap the *oriC*-proximal reporter (Fig. 2). Introducing P_{sirA}-*sirA* back into the chromosome at an ectopic locus in the Δ*sirA* mutant restored *oriC* trapping to levels indistinguishable from wild-type ($P > 0.5$), indicating that the defect could be specifically attributed to the loss of *sirA* (Fig. 2). In comparison, a Δ*soj* mutant failed to capture an *oriC*-proximal reporter (integrated at −7°) in 19% of sporulating cells, while wild-type failed in less than 1% of cells (Fig. 2), similar to prior reports (Sullivan *et al*., 2009). A Δ*soj* Δ*sirA* double mutant phenocopied the Δ*soj* mutant, consistent with SirA acting in the same pathway as Soj to facilitate *oriC* capture. The nine percent difference between the Δ*soj* and Δ*sirA* mutants was reproducible ($P < 0.001$), indicating that Soj also contributes to the capture of *oriC*s in a SirA-independent manner. The

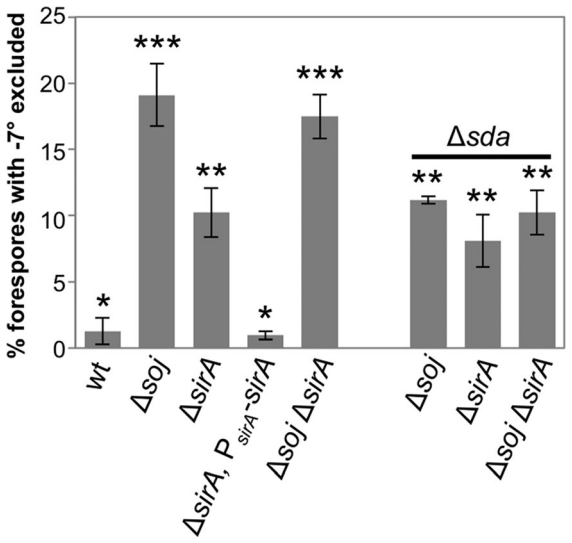

Fig. 2. SirA and Soj act in the same pathway to segregate *oriC* during sporulation. Single cell analysis indicating the average percentage of forespores that fail to capture the origin reporter (−7°) in the forespore during sporulation. Wild-type (BJH103), Δ*soj* (BYD116), Δ*sirA* (BJH090), Δ*sirA*, P_{sirA}-*sirA* (BJH015), Δ*soj* Δ*sirA* (BYD117), Δ*soj* Δ*sda* (BYD470), Δ*sirA* Δ*sda* (BYD472) and Δ*soj* Δ*sirA* Δ*sda* (BYD471). A minimum of 500 cells from each of four biological replicates was counted for each strain (total $n > 2000$ average). Error bars indicate standard deviation from the average of the four trials. The asterisks indicate pairwise comparisons that were statistically indistinguishable ($P > 0.05$, student's *t*-test).

oriC capture defect in the Δ*soj* and Δ*soj* Δ*sirA* double mutants was reduced to 10% when the gene for the DNA replication checkpoint protein, Sda, was also deleted (Fig. 2). In contrast, deletion of *sda* in the Δ*sirA* mutant did not further enhance *oriC* capture in a statistically significant way ($P > 0.05$) (Fig. 2); at the same time we do not exclude the possibility that the slight enhancement of *oriC* capture seen in the Δ*sirA* Δ*sda* mutant compared to the Δ*sirA* mutant represents a real biological difference. Synthesis of Sda delays sporulation in cells that are actively initiating DNA replication (Murray and Errington, 2008). Therefore, these results suggest that the fate of the nine percent of *oriC*s that depend on Soj but not SirA may relate to the replication status of this subset of cells, although we did not investigate this observation further.

A wild-type interaction between SirA and Soj is not required for SirA-dependent oriC *capture*

Our data indicate that SirA and Soj act in the same pathway to facilitate *oriC* segregation in 10% of cells (Fig. 2). To assess if SirA might interact directly with Soj to facilitate *oriC* segregation, we performed a bacterial two-hybrid (B2H) assay. A positive interaction was observed between SirA-T18 and T25-Soj that was

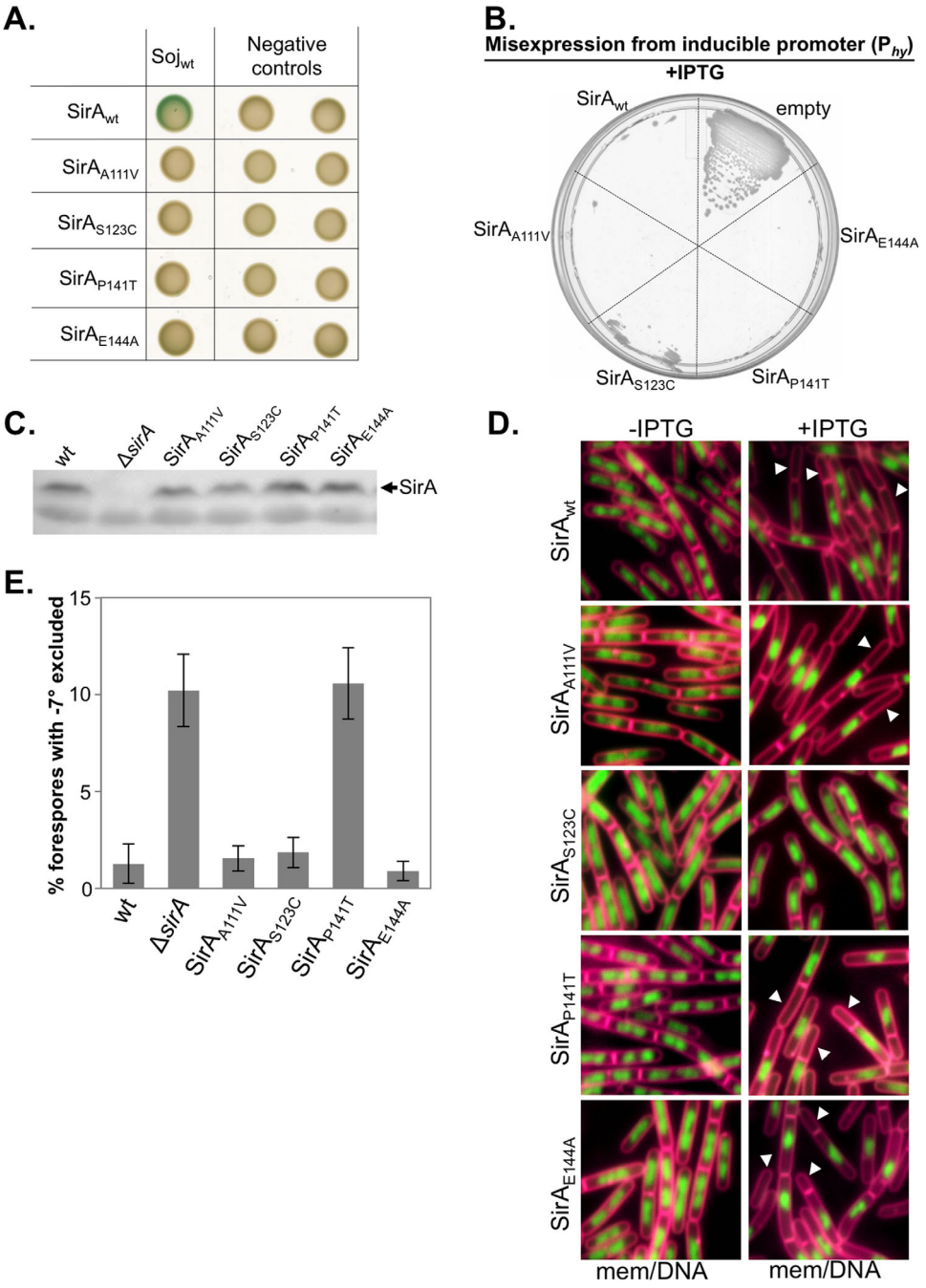

Fig. 3. Identification and characterization of SirA variants that exhibit loss of interaction with Soj.
A. B2H between Soj and SirA (CYD286) or Soj and each of the following SirA variants: SirA$_{A111V}$ (CYD742), SirA$_{S123C}$ (CYD765), SirA$_{P141T}$ (CYD711), SirA$_{E144A}$ (CYD736). Negative controls: empty partner vector with wild-type SirA or the indicated SirA variant (column 1) or Soj with the empty partner vector (column 2).
B. Growth of strains harboring P$_{hy}$-*sirA* (BYD036), P$_{hy}$-*sirA$_{A111V}$* (BYD288), P$_{hy}$-*sirA$_{S123C}$* (BYD295), P$_{hy}$-*sirA$_{P141T}$* (BYD283), P$_{hy}$-*sirA$_{E144A}$* (BYD292) or P$_{hy}$-*empty* (BAM075) following misexpression.
C. Western blot analysis using α-SirA antibody on samples taken 2 h after sporulation by resuspension. Wild-type (BJH103), Δ*sirA* (BJH090), *sirA$_{A111V}$* (BYD306), *sirA$_{S123C}$* (BYD310), *sirA$_{P141T}$* (BYD299), *sirA$_{E144A}$* (BYD308).
D. The same misexpression strains listed in B were grown in CH liquid media 1.5 h after the addition of 1mM IPTG. Cell membranes were stained with FM4-64 (pseudocolored pink) and DNA with DAPI (pseudocolored green). White arrowheads indicate example anucleate cells.
E. Single cell analysis indicating the average percentage of forespores that fail to capture the origin reporter (−7°) in the forespore during sporulation using the same strains listed in C. A minimum of 500 cells from each of four biological replicates was counted for each strain (total $n > 2000$ average). Error bars indicate standard deviation from the average of the four trials. The wild-type and delta *sirA* data from Fig. 2 were replotted to aid comparison. Only the Δ*sirA* mutant and *sirA$_{P141T}$* differ significantly from wild-type.

Table 1. Identification of SirA variants that do not interact with Soj in a B2H assay.

SirA variants exhibiting loss of interaction with Soj

sirA	Variant	Growth
CTG→CCG	L28P	R
CGG→CCG	R64P	R
TTA→TTC	L69F	R
ATA→AAA	I83K	R
TCG→CCG	S106P	R
TTC→TAC	F115Y	R
CCT→CTT	P124L	R
CAA→CTA	Q30L	S
CAG→CAC	Q41H	S
GCA→GTA	A111V	S
AGC→TGC	S123C	S
CCG→ACG	P141T	S
GAA→GCA	E144A	S

Growth refers to the resistance (R), or sensitivity (S) of the cells to SirA-mediated growth inhibition following misexpression from an IPTG inducible promoter (P_{hy}). Each of the misexpression constructs was integrated in single copy at the *amyE* locus.

absent in the negative controls (Fig. 3A). To test if the interaction between SirA and Soj was important for *oriC* capture in vivo, we first screened for SirA variants that exhibited a loss of interaction with Soj. To obtain such variants, we introduced a mutagenized pool of *sirA* PCR products into a B2H plasmid to generate a SirA-T18 pool, and transformed this plasmid pool into *E. coli* reporter cells harboring the B2H partner plasmid, T25-Soj. Next we screened for SirA variants that showed loss of interaction with Soj in the B2H assay. *sirA* alleles that appeared full-length in a PCR test were sequenced, and alleles encoding premature stop codons or multiple mutations were eliminated, leaving 13 candidates (Table 1).

SirA is natively expressed only during sporulation and misexpression (forcing expression during vegetative growth by placing under the control of an IPTG-inducible promoter on the chromosome) inhibits DnaA activity and prevents colony formation on plates (Wagner *et al*., 2009), a phenotype that is not dependent on Soj (Supporting Information Fig. S1). Therefore, we screened for properly folded proteins using misexpression. Seven of the loss-of-interaction mutants did not inhibit DnaA activity, as judged by growth on media containing inducer (Table 1) and were excluded from further analysis since we were unable to assess if they were properly folded. The remaining six mutants phenocopied the wild-type *sirA* vegetative misexpression phenotype (Table 1), suggesting the proteins were not misfolded.

Next we performed the chromosome organization assay on strains harboring $SirA_{A111V}$, $SirA_{S123C}$, $SirA_{P141T}$, or $SirA_{E144A}$. These variants were initially chosen because they showed loss-of-interaction with Soj (Fig. 3A), prevented growth on plates when misexpressed (Fig. 3B), clustered in residues distal to the described DnaA-SirA interaction interface implicated in regulation of DnaA (Jameson *et al*., 2014) (Supporting Information Fig. S2), and exhibited comparable levels of SirA protein compared to wild-type when expressed from the native locus (Fig. 3C). When we investigated the membrane and nucleoid phenotypes associated with vegetative misexpression, $SirA_{A111V}$, $SirA_{P141T}$, and $SirA_{E144A}$ appeared indistinguishable from the control strain misexpressing wild-type SirA, including the generation of anucleate cells (Fig. 3D). However, $SirA_{S123C}$ displayed no obvious signs of inhibited DNA replication, and instead exhibited slightly curved cells or cell poles (Fig. 3D). After 150 min induction, cells expressing $SirA_{S123C}$ exhibited hooked poles, bent filaments, and signs of lysis (Supporting Information Fig. S3). The nucleoids in these cells showed no obvious indications of replication inhibition, suggesting the mechanism leading to cell killing in this strain is distinct from the other three loss-of-interaction variants.

Cells expressing $SirA_{A111V}$, $SirA_{S123C}$, and $SirA_{E144A}$ in place of wild-type SirA captured the *oriC* reporter at levels statistically indistinguishable from wild-type (Fig. 3E). In contrast, the $SirA_{P141T}$ variant phenocopied the Δ*sirA* mutant, failing to capture *oriC* in 10% of sporulating cells (Fig. 3E). From these data we conclude that a wild-type interaction between SirA and Soj is not required for SirA-dependent *oriC* capture and that $SirA_{P141}$ appears to be critical for wild-type SirA activity. Moreover, since $SirA_{P141T}$ can still inhibit DNA replication (Table 1, Fig. 3B and D), these results suggest that the *oriC* capture function of SirA comprises a genetically separable and distinct activity.

SirA facilitates oriC *capture independent of its ability to inhibit DNA replication*

To further test the hypothesis that SirA's ability to inhibit DnaA activity was independent from SirA's observed role in *oriC* segregation, we generated two *sirA* variants, $SirA_{F14A}$ and $SirA_{Y51A}$, which are defective in their ability to inhibit DnaA. $SirA_{F14A}$ has an amino acid substitution at the described interaction interface between SirA and DnaA and was previously shown to be defective in the ability to inhibit DnaA activity in vivo (Jameson *et al*., 2014). Since $SirA_{Y51}$ is also located at the SirA-DnaA interaction interface (Jameson *et al*., 2014), we predicted a substitution in Y51 would also result in a loss-of-function phenotype. Compared to wild-type SirA, both $SirA_{F14A}$ and $SirA_{Y51A}$ showed reduced interaction with full-length DnaA in a B2H assay (Fig. 4A). In addition,

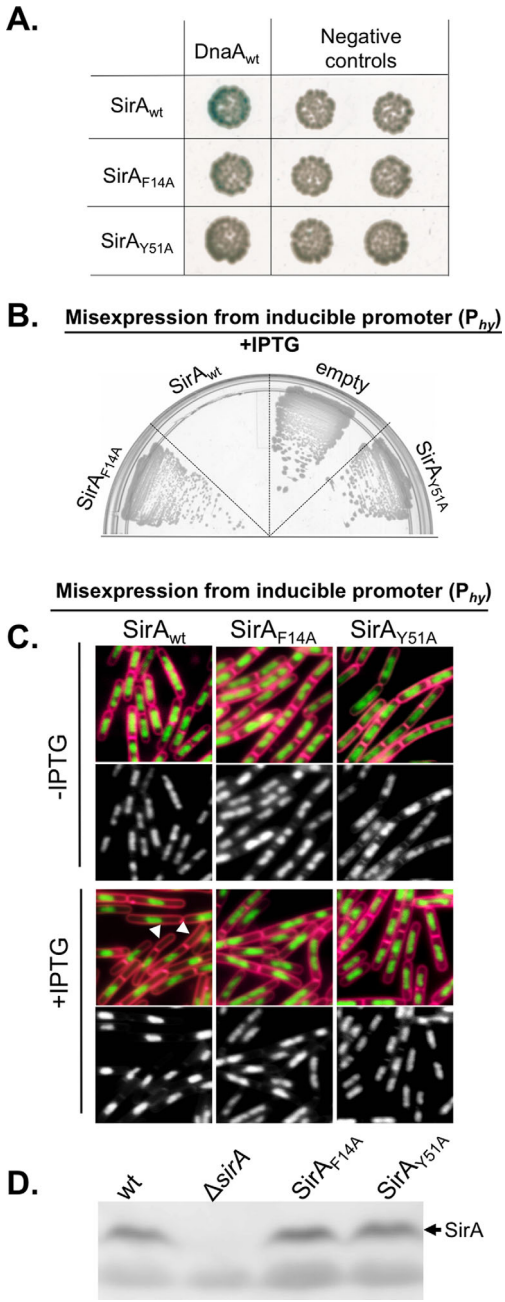

Fig. 4. SirA$_{F14A}$ and SirA$_{Y51A}$ exhibit reduced capacities to inhibit DNA replication.
A. B2H assay between DnaA and SirA (CYD050), DnaA and SirA$_{F14A}$ (CYD823), and DnaA and SirA$_{Y51A}$ (CYD051). Negative controls: empty partner vector with wild-type SirA or the indicated SirA variant (column 1) or DnaA with the empty partner vector (column 2).
B. Growth of strains harboring P$_{hy}$-*sirA* (BYD036), P$_{hy}$-*sirA$_{F14A}$* (BYD462), P$_{hy}$-*sirA$_{Y51A}$* (BYD463) or P$_{hy}$-*empty* (BAM075) following misexpression.
C. The same misexpression strains grown in CH liquid media 1.5 h after the addition of 1 mM IPTG. Cell membranes were stained with FM4-64 (pseudocolored pink) and DNA with DAPI (pseudocolored green). White arrowheads indicate example anucleate cells.
D. Western blot analysis using α-SirA antibody on samples taken 2 h after sporulation by resuspension. Wild-type (BJH103), Δ*sirA* (BJH090), *sirA$_{F14A}$* (BYD302), *sirA$_{Y51A}$* (BYD067).

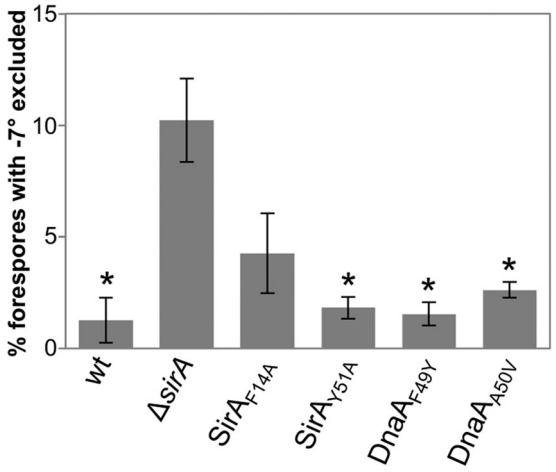

Fig. 5. SirA facilitates *oriC* capture independent of its ability to inhibit DNA replication. Single cell analysis indicating the average percentage of forespores that fail to capture the origin reporter (−7°) in the forespore during sporulation. Wild-type (BJH103), Δ*sirA* (BJH090), *sirA$_{F14A}$* (BYD302), *sirA$_{Y51A}$* (BYD067), *dnaA$_{F49Y}$* (BYD073), *dnaA$_{A50V}$* (BYD303). A minimum of 500 cells from each of four biological replicates was counted for each strain (total $n > 2000$ average). Error bars indicate standard deviation from the average of the four trials. The data for wild-type and Δ*sirA* are identical to those in Fig. 2. The asterisks indicate pairwise comparisons that were statistically indistinguishable ($P > 0.05$, student's *t*-test).

cells misexpressing SirA$_{F14A}$ or SirA$_{Y51A}$ during vegetative growth grew well on plates (Fig. 4B) and did not generate anucleates in liquid culture (Fig. 4C). These results indicate that SirA$_{F14A}$ and SirA$_{Y51A}$ are perturbed in their ability to inhibit DNA replication.

Based on the observation that the DNA replication and *oriC* capture phenotypes were uncoupled in cells expressing SirA$_{P141T}$, we hypothesized that SirA$_{F14A}$ and SirA$_{Y51A}$ would still be able to facilitate *oriC* capture. To test this hypothesis, we replaced native *sirA* with alleles encoding either SirA$_{F14A}$ or SirA$_{Y51A}$ at the native locus. Western blot analysis indicated that variants were stable and expressed at levels indistinguishable from those in wild-type (Fig. 4D). Next, we tested the ability of the variants to facilitate *oriC* capture in the single cell trapping assay (Sullivan *et al.*, 2009). The SirA$_{Y51A}$ variant supported *oriC* capture at levels statistically indistinguishable from wild-type ($P > 0.05$) (Fig. 5). The SirA$_{F14A}$ variant produced a more intermediate phenotype, although it supported capture of the *oriC*-proximal reporter at levels more similar to wild-type than the Δ*sirA* mutant (4% vs. 10%) (Fig. 5). These results further suggest that SirA's role in *oriC* capture can be uncoupled from its ability to inhibit DNA replication initiation.

Although cells misexpressing SirA$_{Y51A}$ and SirA$_{F14A}$ during vegetative growth exhibited phenotypes consistent with a reduced ability to inhibit DnaA-dependent

replication initiation (Fig. 4B and C), it is possible the variants retained sufficient activity to inhibit DNA replication initiation during sporulation. Therefore, we extended our analysis to test *oriC* capture in cells harboring variants of DnaA ($DnaA_{F49Y}$ and $DnaA_{A50V}$) previously shown to be insensitive to SirA misexpression (Rahn-Lee *et al.*, 2011). We replaced wild-type *dnaA* with alleles encoding $DnaA_{F49Y}$ and $DnaA_{A50V}$ (markerless replacement of the wild-type gene at the native locus) and tested the ability of cells to resist the effects of SirA misexpression. Cells possessing either $DnaA_{F49Y}$ or $DnaA_{A50V}$ grew indistinguishably from wild-type during vegetative growth (Fig. 6A) and possessed wild-type nucleoid morphology before SirA induction (Fig. 6B), indicating that the variants were functional with respect to supporting DNA replication initiation in vivo. Both DnaA variants were also resistant to misexpression of SirA as judged by both growth on plates (Fig. 6A) and nucleoid morphology (Fig. 6B). These results confirm prior findings that cells utilizing $DnaA_{F49Y}$ or $DnaA_{A50V}$ are indeed resistant to SirA's ability to inhibit DNA replication initiation (Rahn-Lee *et al.*, 2011). Moreover, the variants did not detectably interact with wild-type SirA in a B2H assay (Fig. 6C), consistent with the loss-of-interaction observed in a yeast two-hybrid assay (Rahn-Lee *et al.*, 2011).

To test if cells utilizing $DnaA_{F49Y}$ or $DnaA_{A50V}$ were compromised in *oriC* segregation, we performed the chromosome organization assay in strain backgrounds harboring alleles encoding either $DnaA_{F49Y}$ or $DnaA_{A50V}$ in place of wild-type *dnaA* at the native locus. Both $DnaA_{F49Y}$ and $DnaA_{A50V}$ supported capture of the *oriC*-proximal reporter at levels statistically indistinguishable from wild-type DnaA ($P > 0.05$) (Fig. 5). These results further support the conclusion that SirA's role in *oriC* capture is not dependent on its ability to inhibit DNA replication through its interactions with DnaA Domain I. At the same time, we do not exclude the possibility that SirA promotes *oriC* segregation through another DnaA-dependent mechanism.

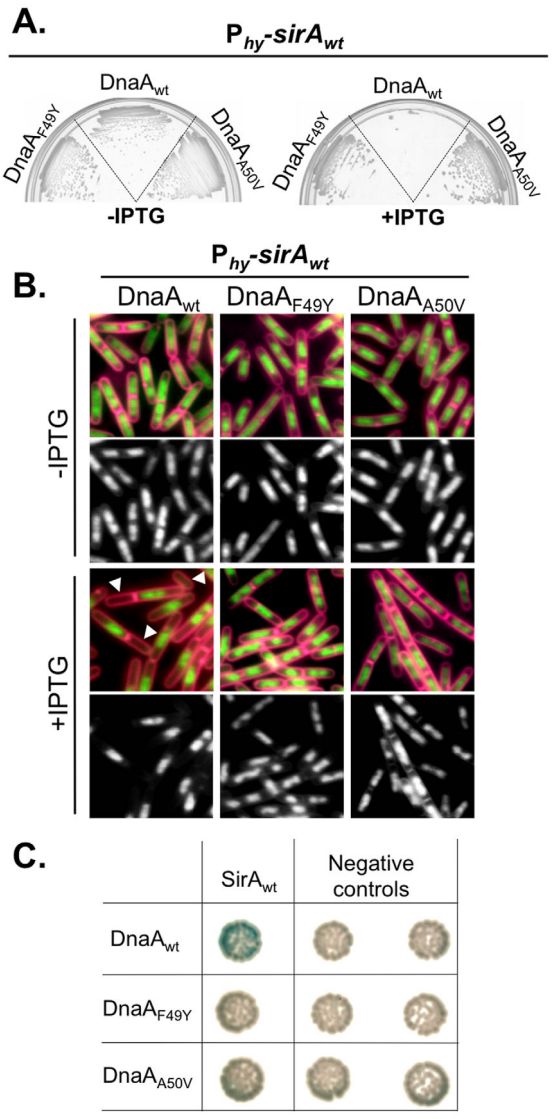

Fig. 6. $DnaA_{F49Y}$ and $DnaA_{A50V}$ are insensitive to SirA-mediated inhibition of DNA replication.
A. Growth of strains harboring P_{hy}-*sirA* in backgrounds encoding wild-type *dnaA* (BYD036), $dnaA_{F49Y}$ (BYD464) or $dnaA_{A50V}$ (BYD465) following misexpression.
B. The same misexpression strains grown in CH liquid media 1.5 h after the addition of 1 mM IPTG. Cell membranes were stained with FM4-64 (pseudocolored pink) and DNA with DAPI (pseudocolored green). White arrowheads indicate example anucleate cells.
C. B2H assay between SirA and DnaA (CYD050), SirA and $DnaA_{F49Y}$ (CYD053), and SirA and $DnaA_{A50V}$ (CYD055). Negative controls: empty partner vector with wild-type DnaA or the indicated DnaA variant (column 1) or SirA with the empty partner vector (column 2).

Residues near the C-terminus of SirA and in DnaA domain III promote interaction between the two proteins

Our data suggest that the DnaA Domain I interaction is not required for *oriC* segregation, and we identified one variant, $SirA_{P141T}$, that supported DNA replication but not *oriC* segregation. Since this substitution occurred in the extreme C-terminus of SirA in a region distal to the described SirA-DnaA interaction interface (Supporting Information Fig. S2), we hypothesized that this second region of SirA might interact with a distinct region of DnaA to promote *oriC* segregation. We were unable to assess the possibility of a second interaction interface using known data, as the SirA-DnaA co-crystal structure could only be obtained using DnaA Domain I (Jameson *et al.*, 2014). Moreover, the suppressor selection utilized to identify DnaA residues important for interaction relied

Table 2. Residues outside the characterized SirA-DnaA interface promote interaction between the two proteins.

DnaA variants exhibiting gain of interaction with $SirA_{Y51A}$

dnaA	Variant
ACT→AAT	T116N
TTT→TCT	F120S
ATC→ACC	I122T
CAT→GAT	H130D
GTA→GGA	V136A
AAA→AAT	K197N
GAT→GTT	D215V
CCG→CTG	P255L
GGA→AGA	G268R

SirA variants exhibiting gain of interaction with $DnaA_{A50V}$

sirA	Variant
ATT→GTT	I103V
ACG→ATG	T113M
GTG→ATG	V118M
AAA→AAT	K121N
CCG→ACG	P141T

Identification of DnaA and SirA variants that result in gain of interaction with $SirA_{Y51A}$ and $DnaA_{A50V}$, respectively, in a B2H assay.

upon the ability of SirA to inhibit DNA replication (Rahn-Lee *et al.*, 2011), which our data indicate is a genetically separable activity. Therefore, we designed two genetic screens to identify SirA and DnaA residues that contribute to interaction between the two full-length proteins.

To identify residues of DnaA important for interaction with SirA, we performed a gain-of-interaction screen based on the observation that $SirA_{Y51A}$ and wild-type DnaA do not detectably interact in the B2H assay (Fig. 4A). We mutagenized *dnaA* and screened for DnaA variants that showed restored interaction with $SirA_{Y51A}$ (Table 2 and Supporting Information Fig. S4). Unexpectedly, each of the nine variants we identified, $DnaA_{T116N}$, $DnaA_{F120S}$, $DnaA_{I122T}$, $DnaA_{H130D}$, $DnaA_{V136A}$, $DnaA_{K197N}$, $DnaA_{D215V}$, $DnaA_{P255L}$, and $DnaA_{G268R}$ possessed substitutions in DnaA Domain III (Table 2 and Supporting Information Fig. S5), a region outside of the known SirA-DnaA interaction interface (Jameson *et al.*, 2014). Of note, $DnaA_{F120}$, $DnaA_{I122}$, and $DnaA_{H130}$ cluster to a region of DnaA Domain III previously implicated in the toxicity bypass associated with induced expression of Soj_{G12V}, a constitutive monomer of Soj that also shows gain of interaction with wild-type DnaA (Scholefield *et al.*, 2012). These results could suggest SirA and Soj are capable of targeting the same region of DnaA, although we do not exclude other possibilities.

In a complementary approach, we took advantage of the fact that wild-type SirA and $DnaA_{A50V}$ do not interact in the B2H assay (Fig. 6C) to identify regions of SirA important for SirA-DnaA interaction. We mutagenized *sirA* and screened for SirA variants that restored interaction with $DnaA_{A50V}$ (Table 2 and Supporting Information Fig. S4). Surprisingly, all of the gain-of-interaction variants we identified ($SirA_{I103V}$, $SirA_{T113M}$, $SirA_{V118M}$, $SirA_{K121N}$, and $SirA_{P141T}$) mapped to a region of SirA distal to the characterized SirA-DnaA Domain I binding interface (Table 2 and Supporting Information Fig. S2). Taken together, the location of the variants identified in the two gain-of-interaction screens are consistent with the idea that residues in SirA's C-terminus interact directly with DnaA Domain III.

Of note, $SirA_{P141T}$ was also identified in the SirA-Soj loss-of-interaction screen (Table 1 and Fig. 3), and each of the SirA-$DnaA_{A50V}$ gain-of-interaction variants identified also exhibited a loss of interaction with Soj in a B2H assay (Fig. 7A). Moreover, with the exception of $SirA_{P141T}$ (Fig. 3E) and $SirA_{T113M}$ (which were statistically different from wild-type, $P < 0.05$), each of the variants fully supported wild-type capture of *oriC* (Fig. 7B). None of the variants prevented colony formation on plates when misexpressed, suggesting they did not inhibit DNA replication (Fig. 7C). These data further support the conclusion that SirA's roles in DNA replication and *oriC* segregation are functionally distinct.

Discussion

In bacteria, DNA replication generally takes place at a single *oriC* and is followed by rapid segregation of the newly replicated origin toward the cell pole (or future cell pole) (Fig. 1). The ParABS system, found in a wide-range of both Gram positive and Gram negative bacteria (Livny *et al.*, 2007), has been implicated in the segregation of chromosomes following replication (Badrinarayanan *et al.*, 2015). However, in *B. subtilis*, cells without Soj (ParA) have no detectable defect in chromosome segregation during vegetative growth (Lee and Grossman, 2006) and a majority (>98%) of cells lacking Spo0J (ParB) still effectively partition chromosomes between daughter cells (Ireton *et al.*, 1994). Spo0J becomes critical when chromosome condensation is severely impacted by the absence of a functional SMC complex (Britton *et al.*, 1998), yet the SMC complex is itself only essential during conditions of fast growth (Britton *et al.*, 1998; Moriya *et al.*, 1998), and even an *smc spo0J* double mutant is still viable under slow growth conditions (Britton *et al.*, 1998). Thus, although Spo0J and SMC are clearly important for fidelity, additional mechanisms likely exist to facilitate chromosome segregation.

Recent evidence indicates that in *B. subtilis*, Soj's major function is to regulate DNA replication initiation by interacting directly with DnaA (Murray and Errington,

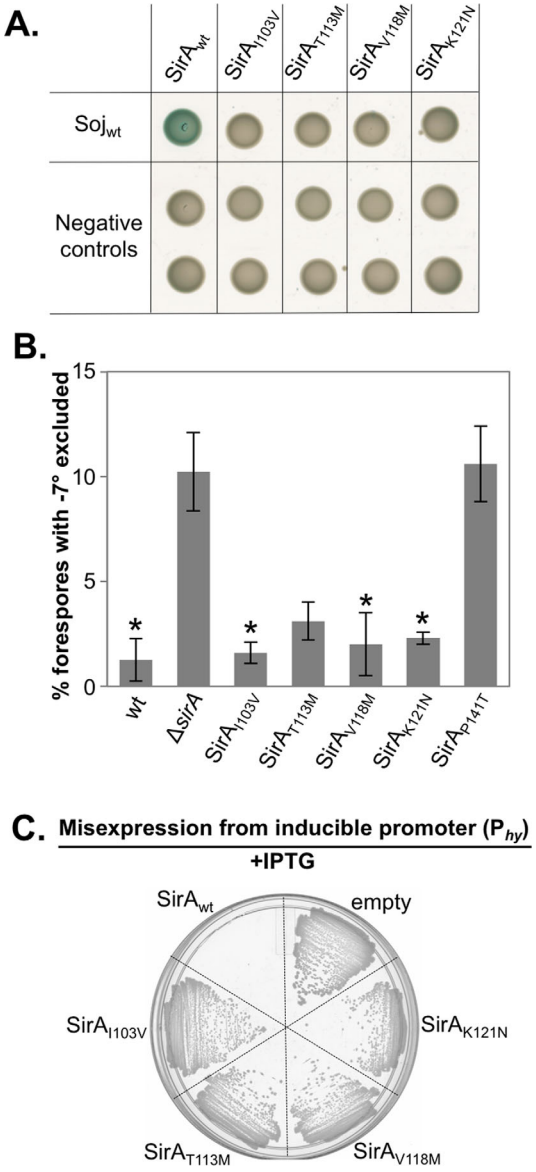

Fig. 7. Variants with mutations in residues outside the characterized SirA-DnaA interface can still segregate *oriC* but cannot inhibit DNA replication.
A. B2H assay between Soj and SirA (CYD286), and Soj and each of the following SirA variants: SirA$_{I103V}$ (CYD1050), SirA$_{T113M}$ (CYD715), SirA$_{V118M}$ (CYD716), SirA$_{K121N}$ (CYD717). Negative controls: empty partner vector with wild-type SirA or the indicated SirA variant (top row) or wild-type Soj with the empty partner vector (bottom row).
B. Single cell analysis indicating the average percentage of forespores that fail to capture the origin reporter (−7°) in the forespore during sporulation. Wild-type (BJH103), Δ*sirA* (BJH090), *sirA$_{I103V}$* (BYD533), *sirA$_{T113M}$* (BYD498), *sirA$_{V118M}$* (BYD499), *sirA$_{K121N}$* (BYD500). A minimum of 2,000 cells from four biological replicates were counted for each strain. The asterisks indicate pairwise comparisons that were statistically indistinguishable ($P > 0.05$, student's *t*-test). The difference between wild-type and *sirA$_{T113M}$* was significant ($P = 0.04$). Error bars indicate standard deviation from the average of the four trials. The data for wild-type, Δ*sirA*, and *sirA$_{P141T}$* are the same as Fig. 3.
C. Growth of strains harboring P$_{hy}$-*sirA* (BYD036), P$_{hy}$-*sirA$_{I103V}$* (BYD549), P$_{hy}$-*sirA$_{T113M}$* (BYD550), P$_{hy}$-*sirA$_{V118M}$* (BYD551), P$_{hy}$-*sirA$_{K121N}$* (BYD552) or P$_{hy}$-*empty* (BAM075) following misexpression.

2008; Scholefield *et al.*, 2012). More specifically, a Soj monomer interacts directly with DnaA Domain III to inhibit DnaA oligomerization until the appropriate cell cycle cue is received for initiation (Scholefield *et al.*, 2012). Spo0J participates in this regulation by stimulating Soj's ATPase activity, thus converting Soj from a dimer to a monomer (Scholefield *et al.*, 2011) (Fig. 1, vegetative). During sporulation, Soj is also important for ensuring that the replication origins of ~20% of sporulating cells are captured in the forespore compartment (Sullivan *et al.*, 2009). It is not known if Soj's *oriC* capture function depends on its ability to regulate DnaA activity, however we observed that about half of the forespores that fail to capture *oriC* in a Δ*soj* mutant can be rescued by deleting *sda* (the percentage of *oriC*s out of forespore decreases from ~20% to ~10%) (Fig. 2). Since Sda executes the sporulation block imposed on actively initiating cells (Veening *et al.*, 2009), this result hints that the *oriC* capture defect may relate to the association of DnaA with *oriC*.

There is some precedence for DnaA affecting *oriC* positioning. In *Caulobacter crescentus*, which requires a functioning ParABS system for *oriC* segregation (Mohl and Gober, 1997; Lim *et al.*, 2014), DnaA has been shown to promote *oriC* segregation independent of its role in initiating DNA replication (Mera *et al.*, 2014). This finding raises the interesting possibility that other bacteria might also utilize initiator proteins to facilitate chromosome segregation. How might this occur? One possibility, which is supported by a growing body of data, is that regulators of DNA replication are spatially coupled to proteins that mark the boundaries of cell poles (and future cell poles) such as DivIVA (Lenarcic *et al.*, 2009; Eswaramoorthy *et al.*, 2014) and MinD (Marston *et al.*, 1998). Consistent with this hypothesis, Soj is capable of localizing at/near septa in a manner that depends on MinD (Autret and Errington, 2003; Murray and Errington, 2008).

Restricting replication initiation to the boundaries of poles and future poles would be an efficient way to facilitate *oriC* segregation during vegetative growth (Fig. 1), but it would also pose a new problem for sporulating *B. subtilis*; during sporulation, the cell quarters become the sites where polar division occurs, so positioning of *oriC* at these sites could drastically decrease the probability of *oriC* being captured on the forespore side of the septum. RacA presumably decreases this probability by anchoring the centromere-like element generated by Spo0J bound at *parS* sites at the extreme cell pole in a DivIVA-dependent manner (Ben-Yehuda *et al.*, 2003; Wu and Errington, 2003; Ben-Yehuda *et al.*, 2005). Additionally, MinD was recently shown to act upstream of Soj in *oriC* capture (Kloosterman *et al.*, 2016). Interestingly, GFP-MinD shows a significant redistribution from the

cell quarter toward a subpolar position during sporulation, and the authors of this study propose that MinD is part of a larger polar segregation complex (which includes Soj), that facilitates redistribution of *oriC* from the cell quarter toward the extreme cell pole (Fig. 1) (Kloosterman *et al*., 2016).

In the present study, our goal was to further investigate the relationship between *oriC* segregation and the activity of the DnaA inhibitor SirA (Wagner *et al*., 2009; Rahn-Lee *et al*., 2011; Jameson *et al*., 2014). We found that in addition to inhibiting DNA replication, SirA is also important for chromosome segregation during sporulation. More specifically, we found that 10% of sporulating cells require SirA to capture *oriC* in the forespore (Fig. 2). Epistasis experiments indicate that SirA acts in the same pathway as Soj to facilitate *oriC* segregation (Fig. 2). Intriguingly, Soj and SirA interact in a B2H assay (Figs 3A and 7A); however, since most of the SirA-Soj loss-of-interaction variants remain functional with respect to facilitating *oriC* capture (Figs 3E and 7B), the physiological relevance of this interaction is currently unclear. The G12V substitution in Soj that exhibits gain of interaction with DnaA (Murray and Errington, 2008) occurs at the interface of a Soj dimer and prevents dimer formation (Scholefield *et al*., 2011). Therefore, one speculation is that if SirA and Soj target the same surface on DnaA Domain III (this remains to be determined, see below), Soj and SirA may be capable of forming a heterodimer.

One of the most significant findings in this study is the observation that SirA's ability to inhibit DNA replication through contacts with DnaA Domain I appears to be completely distinct from SirA's role in *oriC* segregation. DnaA variants insensitive to SirA's replication inhibiting activity ($DnaA_{F49Y}$ or $DnaA_{A50V}$) and several SirA variants perturbed in their ability to inhibit DNA replication ($SirA_{Y51A}$, $SirA_{I103V}$, $SirA_{V118M}$, and $SirA_{K121N}$), each exhibit wild-type *oriC* capture phenotypes (Figs 5 and 7B). Reciprocally, we identified one SirA variant ($SirA_{P141T}$) that inhibits DNA replication, yet is unable to support *oriC* capture. Functional analyses of several SirA-DnaA gain-of-interaction variants further suggest that the *oriC* capture function of SirA is mediated through a previously uncharacterized interaction between SirA and DnaA Domain III. Interestingly, we did not identify even a single compensatory substitution that restored interaction at the known interface between in SirA and DnaA Domain I in either of the gain of interaction screens, suggesting the requisite substitutions are rare or may require more than one amino acid change. In addition, although we think it is unlikely since SirA does not interact with wild-type *E. coli* DnaA (Rahn-Lee *et al*., 2011), we also cannot exclude the possibility that the gain of interactions we observe are mediated through one or more *E. coli* proteins acquiring the capacity to bridge the interaction between SirA and DnaA in the B2H.

In the absence of structural data, we are unable to confidently assess if SirA might have the capability to interact with DnaA Domain I and Domain III simultaneously, or if such an interaction would be mutually exclusive (either DnaA Domain I or Domain III). We favor the second model, as all but one of the SirA-DnaA gain-of-interaction variants we identified support *oriC* capture (Fig. 7B), but no longer prevent growth following misexpression (Fig. 7C). We hypothesize that these SirA variants do not kill because they have an increased propensity to interact with Domain III over Domain I.

Several of the substitutions in DnaA Domain III that show gain of interaction with SirA (specifically $DnaA_{F120S}$, $DnaA_{I122T}$, and $DnaA_{H130D}$) map to a surface previously shown to suppress the toxicity associated with overexpression of Soj_{G12V}, a monomeric variant of Soj (Scholefield *et al*., 2012) (Supporting Information Fig. S5). Interestingly, Soj_{G12V} also shows gain of interaction with DnaA (Murray and Errington, 2008). Substitutions obtained in residues in this region of DnaA (A132 and A131) also exhibited overreplication phenotypes that could act as general suppressors of replication inhibition, thus this region of DnaA was not considered a likely location for direct interaction with Soj (Scholefield *et al*., 2012). Residues in this region of DnaA have also been implicated as possible sites of interaction with YabA and DnaD (Cho *et al*., 2008; Scholefield and Murray, 2013)(Fig. 6), two other DnaA regulators that can also inhibit DnaA oligomerization (Bonilla and Grossman, 2012; Scholefield and Murray, 2013). It is feasible that if Soj targets this surface of DnaA, then substitutions that change the Soj-DnaA interaction might also affect DnaD and YabA binding, leading to overreplication.

If SirA targets the same surface of DnaA Domain III as Soj, then why would both SirA and Soj be required to reposition *oriC* toward the extreme cell pole during sporulation (Fig. 8)? Current data does not reveal if SirA acts upstream, downstream, or in parallel with Soj in *oriC* capture. We hypothesize that at some point prior to polar division, Soj is no longer able to perform its function in inhibiting new rounds of DNA replication, perhaps because it is repositioned toward the distal pole via interactions with MinD (Scholefield *et al*., 2011; Kloosterman *et al*., 2016) or because Spo0J is no longer available to stimulate formation of the Soj monomer. In this capacity, SirA could functionally replace Soj (Fig. 8), interacting with DnaA Domain III and thereby inhibiting oligomerization at *oriC* (Fig. 8). SirA could also prevent DnaA from associating with the membrane-associated initiation proteins DnaD/B (Rokop *et al*., 2004), thus keeping *oriC* free to segregate. The additional requirement of Soj for *oriC* capture could also suggest that Soj is required to create a conformation of DnaA favorable

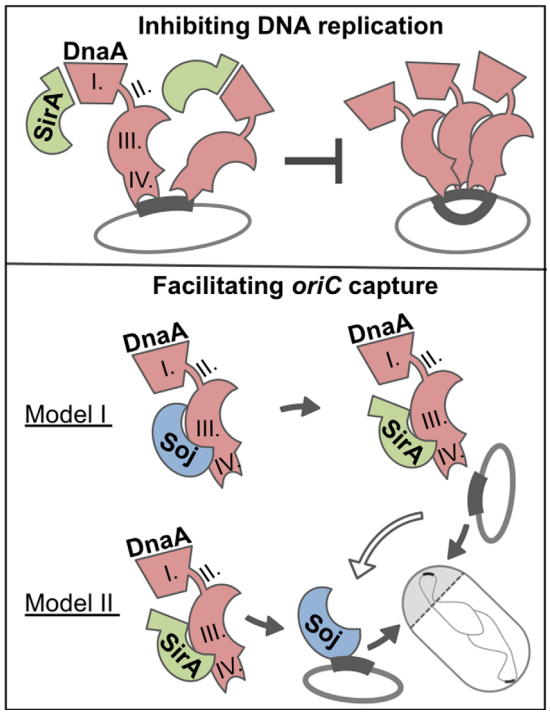

Fig. 8. Models for SirA activity.
SirA inhibits DNA replication through interactions with DnaA Domain I; this activity is not required for *oriC* capture. SirA targets DnaA Domain III to maintain *oriC* in a state favorable for repositioning. In Model I, Soj acts upstream of SirA, generating a conformation of DnaA favorable for SirA association. The association of SirA with DnaA Domain III then permits *oriC* repositioning. In Model II, Soj acts downstream of SirA to facilitate *oriC* capture. Model I does not exclude the possibility that Soj may also be required to facilitate *oriC* capture through an independent, downstream mechanism (open arrow).

for SirA to bind DnaA Domain III (Fig. 8, Model I), and/or that Soj acts downstream of SirA to facilitate *oriC* repositioning through an independent mechanism (Fig. 8, Model I and II). Regardless of the mechanism, we propose that in this capacity, SirA's function is to ensure that the 10% of cells that would otherwise fail to capture *oriC* are able to do so. This 10% decrease may seem small, however since *oriC* capture is critical for successful sporulation (Becker and Pogliano, 2007), having such failsafe mechanisms in place would result in a significant fitness advantage in the face of selective pressures like desiccation.

It is intriguing that Soj and SirA, two different proteins involved in *oriC* positioning, also directly regulate aspects of initiator function. Jacob and Brenner, in their discussion of the replicon model for DNA replication in bacteria, alluded to the possibility of such a connection more than 50 years ago. "In bacteria, a simple and precise system insuring both the regulation of chromosome duplication and the distribution of the two formed chromosomes to the two daughter cells could result from a connection between the chromosome and the bacterial surface; the initiator, for instance, being attached to some specific structure of the cell surface" (Jacob *et al.*, 1963). Although some details of their model turned out to be wrong (for example, elongation between anchored origins does not account for the rapid segregation of chromosomes following initiation), the core idea that interactions among the initiator, the chromosome, and the membrane could help partition chromosomes still remains a valid model. Such a model explains not only the robustness of chromosome segregation observed in model systems, but also hints at how chromosome partitioning may have evolved in early forms of life proliferating through vesiculation and blebbing of membranes (Leaver *et al.*, 2009).

Experimental procedures

General methods

All *B. subtilis* strains were derived from *B. subtilis* 168 or PY79. *E. coli* and *B. subtilis* strains utilized in this study are listed in Supporting Information Table S1. Plasmids are listed in Supporting Information Table S2. Oligonucleotide primers are listed in Supporting Information Table S3. All cloning was carried out in *E. coli* DH5α. *E. coli* strain DHP1 was used for assaying interaction in the B2H. Sporulation was induced by resuspension at 37°C according to the Sterlini-Mandelstam method (Harwood, 1990). For microscopy experiments, all samples were grown in 25 ml CH (Harwood and Cutting, 1990) in 250 ml baffled flasks at 37°C in a shaking waterbath set at 280 rpm. For transformation of *E. coli*, antibiotics were included at the following concentrations when indicated: 100 μg/ml ampicillin, and 25 μg/ml kanamycin. For transformation and selection of *B. subtilis*, antibiotics, when required, were included at the following concentrations: 100 μg/ml spectinomycin, 7.5 μg/ml chloramphenicol, 0.8 μg/ml phleomycin, 10 μg/ml tetracycline, 10 μg/ml kanamycin and 1 μg/ml erythromycin with 25 μg/ml lincomycin.

Microscopy

All samples were grown in CH media overnight at room temperature to mid-exponential, back-diluted to $OD_{600} = 0.008$ in 25 ml CH, and grown at 37°C in a shaking waterbath set at 280 rpm for 1.5 h. When indicated, 1 mM IPTG was added, and cells were grown for an additional 1.5 h. All cells were in mid-exponential growth when images were captured. To capture images, 1 ml of cells were pelleted at 6,010 × g for 1 min in a tabletop microfuge at room temperature. The supernatant was removed by aspiration and the pellet resuspended in ~10 ul PBS containing FM4-64 membrane stain (3 μg/ml) (Life Technologies) and DAPI DNA stain (2 μg/ml) (Molecular Probes). Cells were mounted on glass slides with polylysine treated coverslips immediately before imaging. Fluorescence microscopy was performed with a Nikon Ti-E microscope equipped with a CFI

Plan Apo lambda DM 100X objective, and Prior Scientific Lumen 200 Illumination system, C-FL UV-2E/C DAPI, C-FL GFP HC HISN Zero Shift, C-FL YFP HC HISN Zero Shift, and C-FL Cyan GFP, filter cubes, and a CoolSNAP HQ2 monochrome camera. All images were captured with NIS Elements Advanced Research (version 4.10), and processed with NIS Elements and ImageJ64 (Rasband, 1997-).

Quantitative forespore chromosome trapping assay

Assays were carried out as previously described (Sullivan *et al.*, 2009). An *oriC*-proximal reporter (−7° *yycR*::P_{spoIIQ}-*YFP*) and a right-arm reporter (28° *amyE*::P_{spoIIQ}-*CFP*) were used to assess chromosome organization. Cells were collected and membranes were stained with TMA-DPH (0.02 mM) as described in microscopy. YFP, CFP, and TMA-DPH images were captured 2.5 h after cells were resuspended and grown in sporulation media (Harwood, 1990) at 37°C in a shaking waterbath set at 280 rpm. Images from a minimum of four biological replicates were captured for each strain. To quantitate the number of cells with the forespore reporters trapped in the forespore, the CFP, YFP, and TMA images were pseudocolored and overlaid. Forespores containing detectable signal from YFP, CFP, or both from at least four independent fields ($n > 500$ cells per trial) were counted manually for each biological replicate, adjusting brightness to ensure that even cells with faint signal were counted. Forespores failing to capture either reporter were generally <1% and were not included in the counts for −7° reporter excluded. The average percentage and standard deviation of forespores with CFP signal only (indicating that the −7 *oriC*-proximal reporter was not captured in the forespore) were plotted using Microsoft Excel. The statistical significance between samples (P-value) was determined using an unpaired Student's *t*-test.

Bacterial two-hybrid assay (B2H), general methods

Bacterial two hybrids were performed essentially as described (Karimova *et al.*, 1998) with the following modifications: cloning was carried out in the presence of 0.2% glucose (w/v) in addition to antibiotics. *E. coli* strain DHP1 harboring the relevant pairwise interactions were grown to exponential phase in LB with 0.2% glucose (w/v), ampicillin (50 μg/ml), and kanamycin (25 μg/ml). Samples were normalized by OD_{600} and five μl of each culture spotted on M9-glucose minimal media plates containing 250 μM isopropyl-β-D-thiogalactopyranoside (IPTG), 40 μg/ml 5-bromo-4-chloro-3-indolyl-β-D-galactopyranoside (X-Gal), ampicillin (50 μg/ml), and kanamycin (25 μg/ml). Plates were incubated at room temperature in the dark for 50 to 70 h prior to image capture.

Screen for SirA variants that exhibited a loss of interaction with Soj

The loss-of-interaction screen was performed by B2H assay (see above). Soj was fused to C-terminus of the *cyaA* T25 domain (T25-Soj). SirA was fused to N-terminus of the *cyaA* T18 domain (SirA-T18). *E. coli* strain DHP1 was cotransformed with a plasmid encoding wild-type T25-Soj and a ligation reaction between a mutagenized pool of *sirA* PCR products digested with SphI and BamHI and pCH363 cut with SphI and BamHI (to generate SirA-T18 fusions). The *sirA* gene was mutagenized by PCR using the Genemorph II random DNA mutagenesis kit (Agilent Technologies). The co-transformations were plated on LB solid media (1.5% bacto-agar (w/v)) supplemented with 0.2% glucose (w/v), ampicillin (50 μg/ml), and kanamycin (25 μg/ml). To screen for loss-of-interaction variants, ∼2,000 colonies were patched onto M9-glucose minimal media plates supplemented with IPTG (250 μM), X-Gal (40 μg/ml), ampicillin (50 μg/ml), and kanamycin (25 μg/ml). Patches that appeared white were rescreened on M9-glucose minimal media plates containing IPTG (250 μM), X-Gal (40 μg/ml), ampicillin (50 μg/ml), and kanamycin (25 μg/ml) to reduce the number of false negatives. Approximately 12% of the clones screened showed a loss of interaction between SirA and Soj. PCR with primers oYD70 and oYD354 was used to eliminate loss-of-interaction candidates that lacked a *sirA* insert of the appropriate size in the SirA-T18 plasmid, reducing the number of candidates to 42. These candidates were sequenced to eliminate candidates possessing premature stop codons or multiple mutations, reducing the number of candidates to 13. To exclude SirA variants that might be misfolded, each candidate allele was PCR amplified with OYD362 and OYD363, cloned into the HindIII/NheI site of an inducible misexpression vector (see Supporting Information text for details) and growth was assessed as described.

Screen for SirA variants that exhibit a gain of interaction with $DnaA_{A50V}$

The gain-of-interaction screen was performed by first co-transforming *E. coli* strain DHP1 with a plasmid encoding $DnaA_{A50V}$-T25 and a pool of mutagenized *sirA*-T18 ligation products. The *sirA* gene was mutagenized by PCR using the Genemorph II random DNA mutagenesis kit (Agilent Technologies). Cotransformation was selected for on LB plates supplemented with 0.2% glucose (w/v), ampicillin (50 μg/ml), and kanamycin (25 μg/ml). Gain-of-interaction variants were identified by screening on M9-glucose minimal media plates supplemented with IPTG (250 μM), X-Gal (40 μg/ml), ampicillin (50 μg/ml), and kanamycin (25 μg/ml). Plasmids encoding candidates were used as the template to amplify *sirA* region using oYD70 and oYD354, and each PCR product was sequenced by using oYD116 and oYD117 to determine the identity of the associated mutations.

Screen for DnaA variants that exhibit a gain of interaction with $SirA_{Y51A}$

The gain-of-interaction screen was performed by first co-transforming cells with a plasmid encoding $SirA_{Y51A}$-T18 and a pool of mutagenized *dnaA*-T25 ligation products. The co-transformations were plated on LB plates supplemented with 0.2% glucose (w/v), ampicillin (50 μg/ml), and

kanamycin (25 μg/ml) and gain-of-interaction variants were identified by screening patches on M9-glucose minimal media plates supplemented with IPTG (250 μM), X-Gal (40 μg/ml), ampicillin (50 μg/ml), and kanamycin (25 μg/ml). Plasmids encoding gain-of-interaction candidates were used as the template to amplify *dnaA* using oYD46 and oYD47. Each PCR product was sequenced in both directions using oYD296 and oYD297.

Allelic replacement of wild-type sirA *with* sirA *mutants*

The *sirA* mutants were generated through allelic replacement. Briefly, each mutant gene was generated using overlap extension PCR and cloned into the vector pMiniMad, a plasmid harboring a temperature sensitive origin of replication (specific oligonucleotides and details on individual plasmid construction can be found in the Supporting Information text). Each plasmid was then transformed into *B. subtilis* 168 and single-crossover integration was selected by plating cells at 37°C in the presence of erythromycin (1 μg/ml) and lincomycin (25 μg/ml). Six independent colonies were inoculated into six independent 3 ml LB cultures and grown overnight at room temperature in a rotary drum set at 60 rpm. The next day, the cultures were back-diluted 150X in fresh LB, and grown 8 h at room temperature. 100 μl of a 10^{-5} dilution of each culture was plated on 6 independent LB plates, and incubated overnight at 37°C. Ten single colonies from each plate were patched on LB plate and LB plate supplemented with erythromycin (1 μg/ml) and lincomycin (25 μg/ml). After streaking for isolated colonies, genomic DNA was collected from several antibiotic sensitive colonies obtained from each independent culture. The *sirA* region was then PCR-amplified (primer pair oYD006 and oYD007) and strains carrying the desired mutation were identified by sequencing with primer oYD116 and oYD117.

Plate growth assay

B. subtilis strains were streaked on LB plates containing 100 μg/ml spectinomycin and 1 mM isopropyl-β-D-thiogalactopyranoside (IPTG) when indicated. The plates were incubated at 37°C overnight and images were captured on a ScanJet G4050 flatbed scanner (Hewlett Packard) set on medium format mode.

Western blot analysis

To test the stability of SirA variants by western blot analysis, 2 ml cell pellets were collected 2 h after resuspension in sporulation media (Harwood, 1990) and frozen at −80°C until processing. Lysates were generated by resuspending each pellet in 50 μl lysis buffer [20 mM Tris pH 7.5, 10 mM EDTA, 1 mg/ml lysozyme, 10 μg/ml DNase I, 100 μg/ml RNase A, 1mM PMSF] and incubated 15 min at room temperature. Fifty microliter of 2X sample buffer [0.25 M Tris pH 6.8, 4% SDS, 20% glycerol, 10 mM EDTA] containing 10% 2-mercaptoethanol was added and samples were boiled for 5 min. Lysate loads were normalized by OD_{600} values obtained at the time of cell harvest (normalized to $OD_{600} = 1$). Five microliter of each cell lysate was loaded, and proteins were separated on a 4–20% Tris-HCl gradient gels (Lonza). Proteins were transferred to nitrocellulose membrane (Pall) for 1 h at 60 V on an ice bath. Membranes were blocked in PBS [pH 7.4] containing 0.05% Tween-20 and 5% non-fat milk powder (w/v). Membranes were incubated overnight at 4°C with a 1:1,000 dilution of α-SirA peptide antibody (CSKRYGWLNPVKERN, Genscript) in PBS [pH 7.4] containing 0.05% Tween-20 and 5% non-fat milk powder (w/v) and washed. The membranes were then incubated with 1:10,000 dilutions of horseradish peroxidase-conjugated goat anti-rabbit immunoglobulin G secondary antibody (Bio-Rad) in PBS [pH 7.4] containing 0.05% Tween-20 and 5% non-fat milk powder (w/v) for 1 h at room temperature. After washing, blots were incubated with SuperSignal West Femto Chemiluminescent substrate (Thermo) prior to capture in an Amersham Imager 600 (GE Healthcare). All western blots were performed on a minimum of three biological and experimental replicates. Densitometric analysis of the levels compared to the wild-type controls were performed with ImageJ (Rasband, 1997-). Levels of SirA were always within twofold of wild-type for all of the strains examined.

Acknowledgements

We gratefully acknowledge Deborah Siegele for the suggestion to perform gain-of-interaction screens, Grant Shryock for generation of two-hybrid constructs, and members of the Center for Phage Technology and bacterial “supergroup” for helpful feedback on this project.

References

Autret, S., and Errington, J. (2003) A role for division-site-selection protein MinD in regulation of internucleoid jumping of Soj (ParA) protein in *Bacillus subtilis*. *Mol Microbiol* **47**: 159–169.

Badrinarayanan, A., Le, T.B., and Laub, M.T. (2015) Bacterial chromosome organization and segregation. *Annu Rev Cell Dev Biol* **31**: 171–199.

Becker, E.C., and Pogliano, K. (2007) Cell-specific SpoIIIE assembly and DNA translocation polarity are dictated by chromosome orientation. *Mol Microbiol* **66**: 1066–1079.

Ben-Yehuda, S., Rudner, D.Z., and Losick, R. (2003) RacA, a bacterial protein that anchors chromosomes to the cell poles. *Science* **299**: 532–536.

Ben-Yehuda, S., Fujita, M., Liu, X.S., Gorbatyuk, B., Skoko, D., Yan, J., *et al.* (2005) Defining a centromere-like element in *Bacillus subtilis* by Identifying the binding sites for the chromosome-anchoring protein RacA. *Mol Cell* **17**: 773–782.

Bonilla, C.Y., and Grossman, A.D. (2012) The primosomal protein DnaD inhibits cooperative DNA binding by the replication initiator DnaA in *Bacillus subtilis*. *J Bacteriol* **194**: 5110–5117.

Bramkamp, M., Emmins, R., Weston, L., Donovan, C., Daniel, R.A., and Errington, J. (2008) A novel component

of the division-site selection system of *Bacillus subtilis* and a new mode of action for the division inhibitor MinCD. *Mol Microbiol* **70**: 1556–1569.
Britton, R.A., Lin, D.C., and Grossman, A.D. (1998) Characterization of a prokaryotic SMC protein involved in chromosome partitioning. *Genes Dev* **12**: 1254–1259.
Burkholder, W.F., Kurtser, I., and Grossman, A.D. (2001) Replication initiation proteins regulate a developmental checkpoint in *Bacillus subtilis*. *Cell* **104**: 269–279.
Bylund, J.E., Haines, M.A., Piggot, P.J., and Higgins, M.L. (1993) Axial filament formation in *Bacillus subtilis*: induction of nucleoids of increasing length after addition of chloramphenicol to exponential-phase cultures approaching stationary phase. *J Bacteriol* **175**: 1886–1890.
Cho, E., Ogasawara, N., and Ishikawa, S. (2008) The functional analysis of YabA, which interacts with DnaA and regulates initiation of chromosome replication in *Bacillus subtils*. *Genes Genet Syst* **83**: 111–125.
dos Santos, V.T., Bisson-Filho, A.W., and Gueiros-Filho, F.J. (2012) DivIVA-mediated polar localization of ComN, a posttranscriptional regulator of *Bacillus subtilis*. *J Bacteriol* **194**: 3661–3669.
Eswaramoorthy, P., Winter, P.W., Wawrzusin, P., York, A.G., Shroff, H., and Ramamurthi, K.S. (2014) Asymmetric division and differential gene expression during a bacterial developmental program requires DivIVA. *PLoS Genet* **10**: e1004526.
Gerdes, K., Moller-Jensen, J., and Bugge Jensen, R. (2000) Plasmid and chromosome partitioning: surprises from phylogeny. *Mol Microbiol* **37**: 455–466.
Gruber, S., and Errington, J. (2009) Recruitment of condensin to replication origin regions by ParB/SpoOJ promotes chromosome segregation in *B. subtilis*. *Cell* **137**: 685–696.
Harwood, C.R., and Cutting, S.M. (1990) *Molecular Biological Methods for Bacillus*. New York, NY: Wiley.
Hirano, T. (2016) Condensin-based chromosome organization from bacteria to vertebrates. *Cell* **164**: 847–857.
Ireton, K., Gunther, N.W., IV, and Grossman, A.D. (1994) *spo0J* is required for normal chromosome segregation as well as the initiation of sporulation in *Bacillus subtilis*. *J Bacteriol* **176**: 5320–5329.
Jacob, F., Brenner, S., and Cuzin, F. (1963) On the regulation of DNA replication in bacteria. *Cold Spring Harb Symp Quant Biol* **28**: 329–348.
Jameson, K.H., Rostami, N., Fogg, M.J., Turkenburg, J.P., Grahl, A., Murray, H., and Wilkinson, A.J. (2014) Structure and interactions of the *Bacillus subtilis* sporulation inhibitor of DNA replication, SirA, with domain I of DnaA. *Mol Microbiol* **93**: 975–991.
Karimova, G., Pidoux, J., Ullmann, A., and Ladant, D. (1998) A bacterial two-hybrid system based on a reconstituted signal transduction pathway. *Proc Natl Acad Sci USA* **95**: 5752–5756.
Kloosterman, T.G., Lenarcic, R., Willis, C., Roberts, D.M., Hamoen, L.W., Errington, J., and Wu, L.J. (2016) Complex polar machinery required for proper chromosome segregation in vegetative and sporulating cells of *Bacillus subtilis*. *Mol Microbiol* **101**: 333–350.
Leaver, M., Dominguez-Cuevas, P., Coxhead, J.M., Daniel, R.A., and Errington, J. (2009) Life without a wall or division machine in *Bacillus subtilis*. *Nature* **457**: 849–853.
Lee, P.S., and Grossman, A.D. (2006) The chromosome partitioning proteins Soj (ParA) and Spo0J (ParB) contribute to accurate chromosome partitioning, separation of replicated sister origins, and regulation of replication initiation in *Bacillus subtilis*. *Mol Microbiol* **60**: 853–869.
Lemon, K.P., and Grossman, A.D. (2001) The extrusion-capture model for chromosome partitioning in bacteria. *Genes Dev* **15**: 2031–2041.
Lenarcic, R., Halbedel, S., Visser, L., Shaw, M., Wu, L.J., Errington, J., et al. (2009) Localisation of DivIVA by targeting to negatively curved membranes. *EMBO J* **28**: 2272–2282.
Leonard, T.A., Butler, P.J., and Lowe, J. (2005) Bacterial chromosome segregation: structure and DNA binding of the Soj dimer–a conserved biological switch. *EMBO J* **24**: 270–282.
Lewis, P.J., and Errington, J. (1997) Direct evidence for active segregation of *oriC* regions of the *Bacillus subtilis* chromosome and co-localization with the SpoOJ partitioning protein. *Mol Microbiol* **25**: 945–954.
Lim, H.C., Surovtsev, I.V., Beltran, B.G., Huang, F., Bewersdorf, J., and Jacobs-Wagner, C. (2014) Evidence for a DNA-relay mechanism in ParABS-mediated chromosome segregation. *eLife* **3**: e02758.
Livny, J., Yamaichi, Y., and Waldor, M.K. (2007) Distribution of centromere-like *parS* sites in bacteria: insights from comparative genomics. *J Bacteriol* **189**: 8693–8703.
Marston, A.L., Thomaides, H.B., Edwards, D.H., Sharpe, M.E., and Errington, J. (1998) Polar localization of the MinD protein of *Bacillus subtilis* and its role in selection of the mid-cell division site. *Genes Dev* **12**: 3419–3430.
Mera, P.E., Kalogeraki, V.S., and Shapiro, L. (2014) Replication initiator DnaA binds at the *Caulobacter* centromere and enables chromosome segregation. *Proc Natl Acad Sci USA* **111**: 16100–16105.
Miller, A.K., Brown, E.E., Mercado, B.T., and Herman, J.K. (2016) A DNA-binding protein defines the precise region of chromosome capture during *Bacillus* sporulation. *Mol Microbiol* **99**: 111–122.
Mohl, D.A., and Gober, J.W. (1997) Cell cycle-dependent polar localization of chromosome partitioning proteins in *Caulobacter crescentus*. *Cell* **88**: 675–684.
Moriya, S., Tsujikawa, E., Hassan, A.K., Asai, K., Kodama, T., and Ogasawara, N. (1998) A *Bacillus subtilis* gene-encoding protein homologous to eukaryotic SMC motor protein is necessary for chromosome partition. *Mol Microbiol* **29**: 179–187.
Murray, H., and Errington, J. (2008) Dynamic control of the DNA replication initiation protein DnaA by Soj/ParA. *Cell* **135**: 74–84.
Niki, H., Yamaichi, Y., and Hiraga, S. (2000) Dynamic organization of chromosomal DNA in *Escherichia coli*. *Genes Dev* **14**: 212–223.
Patrick, J.E., and Kearns, D.B. (2008) MinJ (YvjD) is a topological determinant of cell division in *Bacillus subtilis*. *Mol Microbiol* **70**: 1166–1179.
Piggot, P.J., and Hilbert, D.W. (2004) Sporulation of *Bacillus subtilis*. *Curr Opin Microbiol* **7**: 579–586.
Rahn-Lee, L., Gorbatyuk, B., Skovgaard, O., and Losick, R. (2009) The conserved sporulation protein YneE inhibits DNA replication in *Bacillus subtilis*. *J Bacteriol* **191**: 3736–3739.

Rahn-Lee, L., Merrikh, H., Grossman, A.D., and Losick, R. (2011) The sporulation protein SirA inhibits the binding of DnaA to the origin of replication by contacting a patch of clustered amino acids. *J Bacteriol* **193**: 1302–1307.

Reyes-Lamothe, R., Nicolas, E., and Sherratt, D.J. (2012) Chromosome replication and segregation in bacteria. *Annu Rev Genet* **46**: 121–143.

Rokop, M.E., Auchtung, J.M., and Grossman, A.D. (2004) Control of DNA replication initiation by recruitment of an essential initiation protein to the membrane of *Bacillus subtilis*. *Mol Microbiol* **52**: 1757–1767.

Schneider CA, Rasband WS, Eliceiri KW, (2012) NIH Image to ImageJ: 25 years of image analysis. *Nat Methods* **9**: 671–675.

Scholefield, G., and Murray, H. (2013) YabA and DnaD inhibit helix assembly of the DNA replication initiation protein DnaA. *Mol Microbiol* **90**: 147–159.

Scholefield, G., Whiting, R., Errington, J., and Murray, H. (2011) Spo0J regulates the oligomeric state of Soj to trigger its switch from an activator to an inhibitor of DNA replication initiation. *Mol Microbiol* **79**: 1089–1100.

Scholefield, G., Errington, J., and Murray, H. (2012) Soj/ParA stalls DNA replication by inhibiting helix formation of the initiator protein DnaA. *EMBO J* **31**: 1542–1555.

Sharpe, M.E., and Errington, J. (1996) The *Bacillus subtilis* soj-spo0J locus is required for a centromere-like function involved in prespore chromosome partitioning. *Mol Microbiol* **21**: 501–509.

Sharpe, M.E., and Errington, J. (1998) A fixed distance for separation of newly replicated copies of *oriC* in *Bacillus subtilis*: implications for co-ordination of chromosome segregation and cell division. *Mol Microbiol* **28**: 981–990.

Sullivan, N.L., Marquis, K.A., and Rudner, D.Z. (2009) Recruitment of SMC by ParB-*parS* organizes the origin region and promotes efficient chromosome segregation. *Cell* **137**: 697–707.

Veening, J.W., Murray, H., and Errington, J. (2009) A mechanism for cell cycle regulation of sporulation initiation in *Bacillus subtilis*. *Genes Dev* **23**: 1959–1970.

Viollier, P.H., Thanbichler, M., McGrath, P.T., West, L., Meewan, M., McAdams, H.H., and Shapiro, L. (2004) Rapid and sequential movement of individual chromosomal loci to specific subcellular locations during bacterial DNA replication. *Proc Natl Acad Sci USA* **101**: 9257–9262.

Wagner, J.K., Marquis, K.A., and Rudner, D.Z. (2009) SirA enforces diploidy by inhibiting the replication initiator DnaA during spore formation in *Bacillus subtilis*. *Mol Microbiol* **73**: 963–974.

Wang, X., Montero Llopis, P., and Rudner, D.Z. (2014a) *Bacillus subtilis* chromosome organization oscillates between two distinct patterns. *Proc Natl Acad Sci USA* **111**: 12877–12882.

Wang, X., Tang, O.W., Riley, E.P., and Rudner, D.Z. (2014b) The SMC condensin complex is required for origin segregation in *Bacillus subtilis*. *Curr Biol* **24**: 287–292.

Wang, X., Le, T.B., Lajoie, B.R., Dekker, J., Laub, M.T., and Rudner, D.Z. (2015) Condensin promotes the juxtaposition of DNA flanking its loading site in *Bacillus subtilis*. *Genes Dev* **29**: 1661–1675.

Wu, L.J., and Errington, J. (2003) RacA and the Soj-Spo0J system combine to effect polar chromosome segregation in sporulating *Bacillus subtilis*. *Mol Microbiol* **49**: 1463–1475.

Supporting information

Additional supporting information may be found in the online version of this article at the publisher's web-site.

Supplementary Information

The DnaA inhibitor SirA acts in the same pathway as Soj (ParA) to facilitate *oriC* segregation during *Bacillus subtilis* sporulation

Yi Duan, Jack D. Huey, and Jennifer K. Herman*
Department of Biochemistry and Biophysics, Texas A&M University, College Station, TX USA
*Address correspondence to jkherman@tamu.edu

SUPPLEMENTARY FIGURE LEGENDS

Figure S1. Soj is not required for SirA to prevent colony formation on the plate. Cells harboring one copy of P_{hy}-*sirA* (BYD036) or the P_{hy} promoter without an insert (BAM075) in a wildtype background or a Δ*soj* background (BYD574 and BYD575 following misexpression.

Figure S2. Misexpression of $SirA_{S123C}$ in liquid culture. Cells harboring one copy of P_{hy}-$sirA_{S123C}$ (BYD295) strains grown in CH liquid media for 1.5 hr (top) and 2.5 hr (bottom) after the addition of 1mM IPTG. Cell membranes were stained with FM4-64 (pseudocolored pink) and DNA with DAPI (pseudocolored green).

Figure S3. Residues outside the characterized SirA-DnaA interface promote interaction between the two proteins. B2H assay between $SirA_{Y51A}$ and wild-type DnaA (CYD051), or $SirA_{Y51A}$ and each of the following DnaA variants: $DnaA_{T116N}$ (CYD602), $DnaA_{F120S}$ (CYD605), $DnaA_{I122T}$ (CYD608), $DnaA_{H130D}$ (CYD611), $DnaA_{V136A}$ (CYD626), $DnaA_{K197N}$ (CYD629), $DnaA_{D215V}$ (CYD632), $DnaA_{P255L}$ (CYD635), $DnaA_{G268R}$ (CYD638). (B) B2H assay between $DnaA_{A50V}$ and wild-type SirA (CYD055), and $DnaA_{A50V}$ and each of the following SirA variants: $SirA_{I103V}$ (CYD168), $SirA_{T113M}$ (CYD169), $SirA_{V118M}$ (CYD172), $SirA_{K121N}$ (CYD173), $SirA_{P141T}$ (CYD175).

Figure S4. SirA-DnaA Domain I crystal structure. Structure from PDB: 4TPS (Jameson *et al*., 2014)). *B. subtilis* DnaA Domain I (pink) and *B. subtilis* SirA (light green). The location of $SirA_{P141T}$ which exhibits gain of interaction with $DnaA_{A50V}$ and loss of interaction with Soj (red). Location of other SirA variants that exhibit loss-of-interaction with Soj (orange). Location of SirA variants (except $SirA_{P141T}$) that exhibit gain of interaction with $DnaA_{A50V}$ (cyan). The location of the $SirA_{E144A}$ substitution is not shown because it is absent in the structure. Location of substitutions exhibiting loss of interaction with wild-type DnaA (bright green). Location of DnaA substitutions that exhibit loss of interaction with wild-type SirA (purple).

Figure S5. **DnaA Domain III crystal structure.** Structure from PDB: 2Z4S (Ozaki *et al*., 2008). *T. maritima* DnaA Domain III (pink). The location of DnaA substitutions that exhibit gain of interaction with $SirA_{Y51A}$ are shown in cyan on the structure and indicated on the sequence alignment by red asterisks. The location of residue changes that confer resistance to Soj_{G12V} misexpression (Scholefield *et al*., 2012) are indicated with filled black triangles on the sequence alignment. The location of residue changes that confer resistance to YabA misexpression (Scholefield & Murray, 2013) are indicated with filled blue circles. The location of residues implicated in DnaD interaction (Cho *et al*., 2008) are indicated with filled black circles.

Table S1. Strains

Strain	Description	Reference/Figure
Parental		
B. subtilis PY79	*Bacillus subtilis* laboratory strain	(Youngman *et al.*, 1983)
B. subtilis 168	*Bacillus subtilis* laboratory strain 168 *trpC2*	BGSC (1A866)
DH5α	*F- endA1 glnV44 thi-1 recA1 relA1 gyrA96 deoR nupG Φ80dlacZΔM15 Δ(lacZYA-argF)U169, hsdR17(r_K^- m_K^+), λ–*	
DHP1	*F-, cya-99, araD139, galE15, galK16, rpsL1 (Strr), hsdR2, mcrA1,mcrB1;*	Thomas Bernhardt
***B. subtilis* PY79**		
BJH015	*spoIIIE36, yycR::*P_{spoIIQ}*-yfp (phleo), amyE::*P_{spoIIQ}*-cfp (cat), sirA::tet, yvbj::sirA (erm)*	This study
BJH090	*spoIIIE36, yycR::*P_{spoIIQ}*-yfp (phleo), amyE::*P_{spoIIQ}*-cfp (cat), sirA::tet*	This study
BJH103	*spoIIIE36, yycR::*P_{spoIIQ}*-yfp (phleo), amyE::*P_{spoIIQ}*-cfp (cat)*	This study
BKE25690	*sda::erm*	BGSC
BYD067	*spoIIIE36, yycR::*P_{spoIIQ}*-yfp (phleo), amyE::*P_{spoIIQ}*-cfp (cat), sirA::*$sirA_{Y51A}$	This study
BYD073	*spoIIIE36, yycR::*P_{spoIIQ}*-yfp (phleo), amyE::*P_{spoIIQ}*-cfp (cat), dnaA::*$dnaA_{F49Y}$	This study
BYD116	*spoIIIE36, yycR::*P_{spoIIQ}*-yfp (phleo), amyE::*P_{spoIIQ}*-cfp (cat), D(soj, spo0J)::spec, pelB::soj- spo0J+ (kan)*	This study
BYD117	*spoIIIE36, yycR::*P_{spoIIQ}*-yfp (phleo), amyE::*P_{spoIIQ}*-cfp (cat), sirA::tet D(soj, spo0J)::spec, pelB::soj- spo0J+ (kan)*	This study
BYD299	*spoIIIE36, yycR::*P_{spoIIQ}*-yfp (phleo), amyE::*P_{spoIIQ}*-cfp (cat), sirA::*$sirA_{P141T}$	This study
BYD302	*spoIIIE36, yycR::*P_{spoIIQ}*-yfp (phleo), amyE::*P_{spoIIQ}*-cfp (cat), sirA::*$sirA_{F14A}$	This study
BYD303	*spoIIIE36, yycR::*P_{spoIIQ}*-yfp (phleo), amyE::*P_{spoIIQ}*-cfp (cat), dnaA::*$dnaA_{A50V}$	This study
BYD306	*spoIIIE36, yycR::*P_{spoIIQ}*-yfp (phleo), amyE::*P_{spoIIQ}*-cfp (cat), sirA::*$sirA_{A111V}$	This study
BYD308	*spoIIIE36, yycR::*P_{spoIIQ}*-yfp (phleo), amyE::*P_{spoIIQ}*-cfp (cat), sirA::*$sirA_{E144A}$	This study
BYD310	*spoIIIE36, yycR::*P_{spoIIQ}*-yfp (phleo), amyE::*P_{spoIIQ}*-cfp (cat), sirA::*$sirA_{S123C}$	This study
BYD470	*spoIIIE36, yycR::*P_{spoIIQ}*-yfp (phleo), amyE::*P_{spoIIQ}*-cfp (cat), D(soj, spo0J)::spec, pelB::soj- spo0J+ (kan), sda::erm*	This study
BYD471	*spoIIIE36, yycR::*P_{spoIIQ}*-yfp (phleo), amyE::*P_{spoIIQ}*-cfp (cat), D(soj, spo0J)::spec, pelB::soj- spo0J+ (kan), sirA::tet, sda::erm*	This study
BYD472	*spoIIIE36, yycR::*P_{spoIIQ}*-yfp (phleo), amyE::*P_{spoIIQ}*-cfp (cat), sirA::tet, sda::erm*	This study
BYD498	*spoIIIE36, yycR::*P_{spoIIQ}*-yfp (phleo), amyE::*P_{spoIIQ}*-cfp (cat), sirA::*$sirA_{T113M}$	This study
BYD499	*spoIIIE36, yycR::*P_{spoIIQ}*-yfp (phleo), amyE::*P_{spoIIQ}*-cfp (cat), sirA::*$sirA_{V118M}$	This study
BYD500	*spoIIIE36, yycR::*P_{spoIIQ}*-yfp (phleo), amyE::*P_{spoIIQ}*-cfp (cat), sirA::*$sirA_{K121N}$	This study
BYD533	*spoIIIE36, yycR::*P_{spoIIQ}*-yfp (phleo), amyE::*P_{spoIIQ}*-cfp (cat), sirA::*$sirA_{I103V}$	This study
B. subtilis 168		
BAM075	*amyE::*P_{hy} *(spec)*	This study

BYD036	*amyE::*P_{hy}*-sirA (spec)*	This study
BYD283	*amyE::*P_{hy}*-sirA*$_{P141T}$ *(spec)*	This study
BYD285	*amyE::*P_{hy}*-sirA*$_{Q30L}$ *(spec)*	This study
BYD286	*amyE::*P_{hy}*-sirA*$_{Q41H}$ *(spec)*	This study
BYD287	*amyE::*P_{hy}*-sirA*$_{L69F}$ *(spec)*	This study
BYD288	*amyE::*P_{hy}*-sirA*$_{A111V}$ *(spec)*	This study
BYD291	*amyE::*P_{hy}*-sirA*$_{I83K}$ *(spec)*	This study
BYD292	*amyE::*P_{hy}*-sirA*$_{E144A}$ *(spec)*	This study
BYD293	*amyE::*P_{hy}*-sirA*$_{R64P}$ *(spec)*	This study
BYD294	*amyE::*P_{hy}*-sirA*$_{F115Y}$ *(spec)*	This study
BYD295	*amyE::*P_{hy}*-sirA*$_{S123C}$ *(spec)*	This study
BYD296	*amyE::*P_{hy}*-sirA*$_{P124L}$ *(spec)*	This study
BYD297	*amyE::*P_{hy}*-sirA*$_{S106P}$ *(spec)*	This study
BYD298	*amyE::*P_{hy}*-sirA*$_{L28P}$ *(spec)*	This study
BYD462	*amyE::*P_{hy}*-sirA*$_{F14A}$ *(spec)*	This study
BYD463	*amyE::*P_{hy}*-sirA*$_{Y51A}$ *(spec)*	This study
BYD464	*amyE::*P_{hy}*-sirA (spec), dnaA::dnaA*$_{F49Y}$	This study
BYD465	*amyE::*P_{hy}*-sirA (spec), dnaA::dnaA*$_{A50V}$	This study
BYD549	*amyE::*P_{hy}*-sirA*$_{I103V}$ *(spec)*	This study
BYD550	*amyE::*P_{hy}*-sirA*$_{T113M}$ *(spec)*	This study
BYD551	*amyE::*P_{hy}*-sirA*$_{V118M}$ *(spec)*	This study
BYD552	*amyE::*P_{hy}*-sirA*$_{K121N}$ *(spec)*	This study
BYD574	*amyE::*P_{hy}*-sirA (spec), D(soj, spo0J)::cat, pelB::soj- spo0J+ (kan)*	This study
BYD575	*amyE::*P_{hy} *(spec), D(soj, spo0J)::cat, pelB::soj- spo0J+ (kan)*	This study
DHP1		
CYD050	*dnaA-T25 (kan), sirA-T18 (amp)*	This study
CYD051	*dnaA-T25 (kan), sirA*$_{Y51A}$*-T18 (amp)*	This study
CYD053	*dnaA*$_{F49Y}$*-T25 (kan), sirA-T18 (amp)*	This study
CYD055	*dnaA*$_{A50V}$*-T25 (kan), sirA-T18 (amp)*	This study
CYD060	*dnaA-T25 (kan), empty-T18 (amp)*	This study
CYD061	*empty-T25 (kan), sirA-T18 (amp)*	This study
CYD062	*empty-T25 (kan), sirA*$_{Y51A}$*-T18 (amp)*	This study
CYD064	*dnaA*$_{F49Y}$*-T25 (kan), empty-T18 (amp)*	This study
CYD066	*dnaA*$_{A50V}$*-T25 (kan), empty-T18 (amp)*	This study
CYD168	*dnaA*$_{A50V}$*-T25 (kan), sirA*$_{I103V}$*-T18 (amp)*	This study
CYD169	*dnaA*$_{A50V}$*-T25 (kan), sirA*$_{T113M}$*-T18 (amp)*	This study
CYD172	*dnaA*$_{A50V}$*-T25 (kan), sirA*$_{V118M}$*-T18 (amp)*	This study
CYD173	*dnaA*$_{A50V}$*-T25 (kan), sirA*$_{K121N}$*-T18 (amp)*	This study
CYD175	*dnaA*$_{A50V}$*-T25 (kan), sirA*$_{P141T}$*-T18 (amp)*	This study
CYD286	*T25-soj (kan), sirA-T18 (amp)*	This study
CYD306	*T25-soj (kan), empty-T18 (amp)*	This study
CYD307	*T25-empty (kan), sirA-T18 (amp)*	This study
CYD602	*dnaA*$_{T116N}$*-T25 (kan), sirA*$_{Y51A}$*-T18 (amp)*	This study
CYD605	*dnaA*$_{F120S}$*-T25 (kan), sirA*$_{Y51A}$*-T18 (amp)*	This study
CYD608	*dnaA*$_{I122T}$*-T25 (kan), sirA*$_{Y51A}$*-T18 (amp)*	This study
CYD611	*dnaA*$_{H130D}$*-T25 (kan), sirA*$_{Y51A}$*-T18 (amp)*	This study
CYD626	*dnaA*$_{V136A}$*-T25 (kan), sirA*$_{Y51A}$*-T18 (amp)*	This study
CYD629	*dnaA*$_{K197N}$*-T25 (kan), sirA*$_{Y51A}$*-T18 (amp)*	This study
CYD632	*dnaA*$_{D215V}$*-T25 (kan), sirA*$_{Y51A}$*-T18 (amp)*	This study
CYD635	*dnaA*$_{P255L}$*-T25 (kan), sirA*$_{Y51A}$*-T18 (amp)*	This study
CYD638	*dnaA*$_{G268R}$*-T25 (kan), sirA*$_{Y51A}$*-T18 (amp)*	This study

CYD711	*T25-soj (kan), sirA$_{P141T}$-T18 (amp)*	This study
CYD715	*T25-soj (kan), sirA$_{T113M}$-T18 (amp)*	This study
CYD716	*T25-soj (kan), sirA$_{V118M}$-T18 (amp)*	This study
CYD717	*T25-soj (kan), sirA$_{K121N}$-T18 (amp)*	This study
CYD718	*T25-empty (kan), sirA$_{P141T}$-T18 (amp)*	This study
CYD722	*T25-empty (kan), sirA$_{T113M}$-T18 (amp)*	This study
CYD723	*T25-empty (kan), sirA$_{V118M}$-T18 (amp)*	This study
CYD724	*T25-empty (kan), sirA$_{K121N}$-T18 (amp)*	This study
CYD736	*T25-soj (kan), sirA$_{E144A}$-T18 (amp)*	This study
CYD737	*T25-empty (kan), sirA$_{E144A}$-T18 (amp)*	This study
CYD742	*T25-soj (kan), sirA$_{A111V}$-T18 (amp)*	This study
CYD743	*T25-empty (kan), sirA$_{A111V}$-T18 (amp)*	This study
CYD765	*T25-soj (kan), sirA$_{S123C}$-T18 (amp)*	This study
CYD770	*T25-empty (kan), sirA$_{S123C}$-T18 (amp)*	This study
CYD823	*dnaA-T25 (kan), sirA$_{F14A}$-T18 (amp)*	This study
CYD824	*empty-T25 (kan), sirA$_{F14A}$-T18 (amp)*	This study
CYD1050	*T25-soj (kan), sirA$_{I103V}$-T18 (amp)*	This study
CYD1055	*T25-empty (kan), sirA$_{I103V}$-T18 (amp)*	This study

Table S2. Plasmids

Plasmid	Description	Reference/Figure/Use
pCH363	*empty-T18 (amp)*	Tom Bernhardt/B2H vector
pDR111	*amyE::P$_{hy}$-empty (spec)*	David Rudner
pKNT25	*empty-T25 (kan)*	Tom Bernhardt/B2H vector
pKT25	*T25-empty (kan)*	Tom Bernhardt/B2H vector
pminiMAD	*ori^{BsTs} (amp) (erm)*	(Kearns & Losick, 2005)
pYD009	*sirA-T18 (amp)*	This study
pYD011	*dnaA-T25 (kan)*	This study
pYD040	*dnaA$_{F49Y}$-T25 (kan)*	This study
pYD042	*dnaA$_{A50V}$-T25 (kan)*	This study
pYD059	*sirA$_{Y51A}$-T18 (amp)*	This study
pYD081	*pminiMAD-dnaA$_{F49Y}$ (amp)*	This study
pYD096	*T25-soj (kan)*	This study
pYD101	*pminiMAD-sirA$_{Y51A}$ (amp)*	This study
pYD102	*amyE::P$_{hy}$-sirA (amp)*	This study
pYD125	*amyE::P$_{hy}$-sirA$_{P141T}$ (amp)*	This study
pYD126	*amyE::P$_{hy}$-sirA$_{Q30L}$ (amp)*	This study
pYD127	*amyE::P$_{hy}$-sirA$_{I83K}$ (amp)*	This study
pYD128	*pminiMAD-sirA$_{P141T}$ (amp)*	This study
pYD129	*pminiMAD-sirA$_{F14A}$ (amp)*	This study
pYD130	*pminiMAD-dnaA$_{A50V}$ (amp)*	This study
pYD131	*amyE::P$_{hy}$-sirA$_{Q41H}$ (amp)*	This study
pYD132	*sirA$_{E144A}$-T18 (amp)*	This study
pYD133	*amyE::P$_{hy}$-sirA$_{E144A}$ (amp)*	This study
pYD134	*amyE::P$_{hy}$-sirA$_{L69F}$ (amp)*	This study
pYD135	*amyE::P$_{hy}$-sirA$_{A111V}$ (amp)*	This study
pYD136	*amyE::P$_{hy}$-sirA$_{R64P}$ (amp)*	This study
pYD137	*pminiMAD-sirA$_{E144A}$ (amp)*	This study
pYD138	*pminiMAD-sirA$_{S123C}$ (amp)*	This study
pYD139	*sirA$_{S123C}$-T18 (amp)*	This study
pYD140	*amyE::P$_{hy}$-sirA$_{S123C}$ (amp)*	This study
pYD141	*amyE::P$_{hy}$-sirA$_{P124L}$ (amp)*	This study
pYD142	*amyE::P$_{hy}$-sirA$_{S106P}$ (amp)*	This study

pYD143	*amyE::P_{hy}-sirA$_{L28P}$ (amp)*	This study
pYD146	*sirA$_{A111V}$-T18 (amp)*	This study
pYD165	*pminiMAD-sirA$_{A111V}$ (amp)*	This study
pYD166	*pminiMAD-sirA$_{I103V}$ (amp)*	This study
pYD167	*pminiMAD-sirA$_{T113M}$ (amp)*	This study
pYD168	*pminiMAD-sirA$_{V118M}$ (amp)*	This study
pYD169	*pminiMAD-sirA$_{K121N}$ (amp)*	This study
pYD170	*amyE::P_{hy}-sirA$_{F115Y}$ (amp)*	This study
pYD171	*amyE::P_{hy}-sirA$_{F14A}$ (amp)*	This study
pYD172	*amyE::P_{hy}-sirA$_{Y51A}$ (amp)*	This study
pYD173	*sirA$_{I103V}$-T18 (amp)*	This study
pYD174	*sirA$_{T113M}$-T18 (amp)*	This study
pYD175	*sirA$_{V118M}$-T18 (amp)*	This study
pYD176	*sirA$_{K121N}$-T18 (amp)*	This study
pYD177	*sirA$_{P141T}$-T18 (amp)*	This study
pYD178	*dnaA$_{T116N}$-T25 (kan)*	This study
pYD179	*dnaA$_{F120S}$-T25 (kan)*	This study
pYD180	*dnaA$_{I122T}$-T25 (kan)*	This study
pYD181	*dnaA$_{H130D}$-T25 (kan)*	This study
pYD182	*dnaA$_{V136A}$-T25 (kan)*	This study
pYD183	*dnaA$_{K197N}$-T25 (kan)*	This study
pYD184	*dnaA$_{D215V}$-T25 (kan)*	This study
pYD185	*dnaA$_{P255L}$-T25 (kan)*	This study
pYD186	*dnaA$_{G268R}$-T25 (kan)*	This study
pYD187	*sirA$_{F14A}$-T18 (amp)*	This study

Table S3. Oligos

Oligo	Sequence 5' to 3'
OJH083	ATGACAGAGAAACAGATTCAAGCTATTACACAACCAATCCCGA
OYD006	CATTGCATGCGTAACACACAGGAAACAGCTATGGAACGTCACTACTATACG
OYD007	GCATGGATCCGAACCGCTACCGACAAAATTTCTTTCTTTCAC
OYD011	GCATGGTACCGAACCGCTACCTTTAAGCTGTTCTTTAATTTCTTT
OYD035	GCATGGATCCGTAACACACAGGAAACAGCTATGGAAAATATATTAGACCTGTG
OYD043	CAATCACGGCTCCCAATGAATATGCCAGAGACTGGCTGGAGTCC
OYD045	TCACGGCTCCCAATGAATTTGTCAGAGACTGGCTGGAGTCCAG
OYD046	AAGCTTGCATGCCTGCAGGT
OYD047	GGTCGGCGGCGTTTGCGTAAC
OYD059	CAGCCAGTCTCTGGCATATTCATTGGGAGCCGTGATTGTTAATG
OYD061	CTGGACTCCAGCCAGTCTCTGACAAATTCATTGGGAGCCGTGA
OYD070	GTGTGGAATTGTGAGCGGATAAC
OYD116	CATTGGACAAGCCTTGAAAAGCAG
OYD117	GTAATCTCCCGAAGCCACAATTTC
OYD122	GCATGGATCCCGGCTTTTTTTAGTATCCACAG
OYD123	GCATGAATTCGTTTGTAAATTTCTCAGAAGACAG
OYD214	TCGGGATTGGTTGTGTAATAGCTTGAATCTGTTTCTCTGTCAT
OYD215	GCATGGATCCTCAATGGACCGTTTTGAGAAAC
OYD216	GCATGAATTCAGGTTTCATTCCCATTTGCATC
OYD254	GCATGGATCCGGGCAGCGGTGTGGGAAAAATCATAGCAATTAC
OYD255	GCATGAATTCTTAGCCATTCGCAGCCACTTCC
OYD276	AGCAATTACGAACCAAAAAGTCGGGGTCGGCAAAACAACGA
OYD277	TCGTTGTTTTGCCGACCCCGACTTTTTGGTTCGTAATTGCT
OYD280	GGTTCTGCTGGTAGATATTGCTCCGCAGGGAAATGCGACAA
OYD281	TTGTCGCATTTCCCTGCGGAGCAATATCTACCAGCAGAACC

OYD296	CCATTATGTAATAGATCATAATCC
OYD297	GACAACTCTGATTAATGCTCC
OYD302	ATCATAATCTTTACGTATTATTTCG
OYD305	GGCTTCGGGAGATTACGAGGTAGAAACGATATTCTTTGAAG
OYD306	CTTCAAAGAATATCGTTTCTACCTCGTAATCTCCCGAAGCC
OYD310	TATGCTCAATCCAAAATATAATTTTGATACTTTTGTCATCG
OYD311	CGATGACAAAAGTATCAAAATTATATTTTGGATTGAGCATA
OYD312	AAAATATACTTTTGATACTTCTGTCATCGGATCTGGAAACC
OYD313	GGTTTCCAGATCCGATGACAGAAGTATCAAAAGTATATTTT
OYD314	TACTTTTGATACTTTTGTCACCGGATCTGGAAACCGATTTG
OYD315	CAAATCGGTTTCCAGATCCGGTGACAAAAGTATCAAAAGTA
OYD316	GATCTGGAAACCGATTTGCAGATGCTGCTTCCCTCGCAGTA
OYD317	TACTGCGAGGGAAGCAGCATCTGCAAATCGGTTTCCAGATC
OYD326	TGATGTGCTTTTGATAGATGTTATTCAATTTTTAGCGGGGA
OYD327	TCCCCGCTAAAAATTGAATAACATCTATCAAAAGCACATCA
OYD328	TGCGCTCACGTTTTGAATGGAGACTTATTACAGATATCACA
OYD329	TGTGATATCTGTAATAAGTCTCCATTCAAAACGTGAGCGCA
OYD330	AACTCTATCCGAGATAATAATGCCGTCGACTTCCGCAATCG
OYD331	CGATTGCGGAAGTCGACGGCATTATTATCTCGGATAGAGTT
OYD354	CTGTTCAGCGCATTGCGCAC
OYD362	ATGCAAGCTTACATAAGGAGGAACTACTATGGAACGTCACTACTATACG
OYD363	AGCTGCTAGCTTAGACAAAATTTCTTTCTTTCAC
OYD364	GCATGCATGCGTAACACACAGGAAA
OYD365	GCATGGATCCGAACCGCTACCGA
OYD366	CGTACCTGATCAAAGAGGAAGCTGCCAATCACTATTTCGGCC
OYD367	GGCCGAAATAGTGATTGGCAGCTTCCTCTTTGATCAGGTACG
OYD368	GCATGGATCCATGGAACGTCACTACTATACG
OYD369	GCATGAATTCCTGCAAATTGTCATGGCGAAC
OYD376	AGCGTTACGGATGGCTAAATACGGTGAAAGAAAGAAATTTT
OYD377	AAAATTTCTTTCTTTCACCGTATTTAGCCATCCGTAACGCT
OYD380	GGTTATGTTTGAGCTGTTTCTAGACTATCATTGGACAAGCC
OYD381	GGCTTGTCCAATGATAGTCTAGAAACAGCTCAAACATAACC
OYD382	GCTGGATTATATTTATAGAAAAGCTTTGCCGAAAGCAAAAG
OYD383	CTTTTGCTTTCGGCAAAGCTTTTCTATAAATATAATCCAGC
OYD384	AGCTGCTAGCTTAGACAAAATTTCTTGCTTTCAC
OYD387	ATGCGTCGACACATAAGGAGGAACTACTATGGAACGTCACTACTATACG
OYD388	AGCTGCATGCTTAGACAAAATTTCTTTCTTTCAC
OYD389	ACAAGCCTTGAAAAGCAGCACTATGAAATGACAGAGAAACA
OYD390	TGTTTCTCTGTCATTTCATAGTGCTGCTTTTCAAGGCTTGT
OYD391	ATGGCTAAATCCGGTGAAAGCAAGAAATTTTGTCTAAAACC
OYD392	GGTTTTAGACAAAATTTCTTGCTTTCACCGGATTTAGCCAT
OYD397	TTACGAGGCAGAAACGATATACTTTGAAGTGTTAAGAAAAG
OYD398	CTTTTCTTAACACTTCAAAGTATATCGTTTCTGCCTCGTAA
OYD399	TTGAAGTGTTAAGAAAAGTATGCCCTTGCTTTTTAGCAATG
OYD400	CATTGCTAAAAAGCAAGGGCATACTTTTCTTAACACTTCAA
OYD401	AGTGTTAAGAAAAGTAAGCCTTTGCTTTTTAGCAATGGATT
OYD402	AATCCATTGCTAAAAAGCAAAGGCTTACTTTTCTTAACACT
OYD403	ACATGATAGAAATTGTGGCTCCGGGAGATTACGAGGCAGAA
OYD404	TTCTGCCTCGTAATCTCCCGGAGCCACAATTTCTATCATGT
OYD405	GGAATCGGTTATGTTTGAGCCGTTTCAAGACTATCATTGGA
OYD406	TCCAATGATAGTCTTGAAACGGCTCAAACATAACCGATTCC
OYD491	TGAAGGAGCACATGATAGAAGTTGTGGCTTCGGGAGATTAC
OYD492	GGGAGATTACGAGGCAGAAATGATATTCTTTGAAGTGTTAA

OYD493	TTAACACTTCAAAGAATATCATTTCTGCCTCGTAATCTCCC
OYD494	CAGAAACGATATTCTTTGAAATGTTAAGAAAAGTAAGCCCT
OYD495	AGGGCTTACTTTTCTTAACATTTCAAAGAATATCGTTTCTG
OYD496	TTCTTTGAAGTGTTAAGAAATGTAAGCCCTTGCTTTTTAGC
OYD497	GCTAAAAAGCAAGGGCTTACATTTCTTAACACTTCAAAGAA
OYD498	GTAATCTCCCGAAGCCACAACTTCTATCATGTGCTCCTTCA
OYD517	CCGGCCGCCAAAGGAAATTCTGACACTTGAAGACAGATTGC
OYD518	GCAATCTGTCTTCAAGTGTCAGAATTTCCTTTGGCGGCCGG
OYD526	GCATGGATCCGAACCGCTACCGACAAAATTTCTTGCTTTCAC
OYD527	ACATGCTGCTTCCCTCGCAGGAGCGGAAGCGCCCGCGAAAG
OYD528	CTTTCGCGGGCGCTTCCGCTCCTGCGAGGGAAGCAGCATGT

PLASMID CONSTRUCTION

Note: for the genotypes listed in strain and plasmid tables, the following abbreviations were used to indicate the conferred antibiotic resistance:

cat – chloramphenicol resistance
erm – erythromycin/lincomycin resistance
kan – kanamycin resistance
phleo - phleomycin resistance
spec – spectinomycin resistance
tet – tetracycline resistance

pYD009 was generated by cloning the PCR product from OYD006 and OYD007 amplification of *Bs*168 genomic DNA into pCH363 (SphI-BamHI).

pYD011 was generated by cloning the PCR product from OYD035 and OYD011 amplification of *Bs*168 genomic DNA into pKNT25 (KpnI-BamHI).

pYD040 was generated with overlap extension PCR. The "UP" product was amplified from *Bs*168 genomic DNA with primer pair OYD035/OYD059. The "DOWN" product was amplified from *Bs168* genomic DNA with primer pair OYD011/OYD043. The two PCR products were used as template for overlap extension PCR with primer pair OYD035/OYD011. The amplified fragment was cut with BamHI and KpnI and cloned into pKNT25 cut with the same enzymes.

pYD042 was generated with overlap extension PCR. The "UP" product was amplified from *Bs*168 genomic DNA with primer pair OYD035/OYD061. The "DOWN" product was amplified from *Bs168* genomic DNA with primer pair OYD011/OYD045. The two PCR products were used as template for overlap extension PCR with primer pair OYD035/OYD011. The amplified fragment was cut with BamHI and KpnI and cloned into pKNT25 cut with the same enzymes.

pYD059 was generated with overlap extension PCR. The "UP" product was amplified from *Bs*168 genomic DNA with primer pair OYD006/OYD214. The "DOWN" product was amplified from *Bs168* genomic DNA with primer pair OYD007/OJH083. The two PCR products were used as template for overlap extension PCR with primer pair OYD006/OYD007. The amplified fragment was cut with BamHI and SphI and cloned into pCH363 cut with the same enzymes.

pYD081 was generated with overlap extension PCR. The "UP" product was amplified from *Bs*168 genomic DNA with primer pair OYD122/OYD059. The "DOWN" product was amplified from *Bs168* genomic DNA with primer pair OYD123/OYD043. The two PCR products were used as template for overlap extension PCR with primer pair OYD122/OYD123. The amplified fragment was cut with BamHI and EcoRI and cloned into pminiMAD cut with the same enzymes.

pYD096 was generated by cloning PCR product from OYD254 and OYD255 amplification of *Bs*168 genomic DNA into pKT25 (BamHI-EcoRI).

pYD101 was generated with overlap extension PCR. The "UP" product was amplified from *Bs*168 genomic DNA with primer pair OYD215/OJH083. The "DOWN" product was amplified from *Bs168* genomic DNA with primer pair OYD216/OYD214. The two PCR products were used as template for overlap extension PCR with primer pair OYD215/OYD216. The amplified fragment was cut with BamHI and EcoRI and cloned into pminiMAD cut with the same enzymes.

pYD102 was generated by cloning PCR product from OYD362 and OYD363 amplification of *Bs*168 genomic DNA into pDR111 (HindIII-NheI).

pYD125 was generated with overlap extension PCR. The "UP" product was amplified from *Bs*168 genomic DNA with primer pair OYD362/OYD377. The "DOWN" product was amplified from *Bs168* genomic DNA with primer pair OYD363/OYD376. The two PCR products were used as template for overlap extension PCR with primer pair OYD362/OYD363. The amplified fragment was cut with HindIII and NheI and cloned into pDR111 cut with the same enzymes.

pYD126 was generated with overlap extension PCR. The "UP" product was amplified from *Bs*168 genomic DNA with primer pair OYD362/OYD381. The "DOWN" product was amplified from *Bs168* genomic DNA with primer pair OYD363/OYD380. The two PCR products were used as template for overlap extension PCR with primer pair OYD362/OYD363. The amplified fragment was cut with HindIII and NheI and cloned into pDR111 cut with the same enzymes.

pYD127 was generated with overlap extension PCR. The "UP" product was amplified from *Bs*168 genomic DNA with primer pair OYD387/OYD383. The "DOWN" product was amplified from *Bs168* genomic DNA with primer pair OYD388/OYD382. The two PCR products were used as template for overlap extension PCR with primer pair OYD387/OYD388. The amplified fragment was cut with SalI and SphI and cloned into pDR111 cut with the same enzymes.

pYD128 was generated with overlap extension PCR. The "UP" product was amplified from *Bs*168 genomic DNA with primer pair OYD368/OYD377. The "DOWN" product was amplified from *Bs168* genomic DNA with primer pair OYD369/OYD376. The two PCR products were used as template for overlap extension PCR with primer pair OYD368/OYD369. The amplified fragment was cut with BamHI and EcoRI and cloned into pminiMAD cut with the same enzymes.

pYD129 was generated with overlap extension PCR. The "UP" product was amplified from *Bs*168 genomic DNA with primer pair OYD215/OYD367. The "DOWN" product was amplified from *Bs168* genomic DNA with primer pair OYD216/OYD366. The two PCR products were used as template for overlap extension PCR with primer pair OYD215/OYD216. The amplified fragment was cut with BamHI and EcoRI and cloned into pminiMAD cut with the same enzymes.

pYD130 was generated with overlap extension PCR. The "UP" product was amplified from *Bs*168 genomic DNA with primer pair OYD122/OYD061. The "DOWN" product was amplified from *Bs168* genomic DNA with primer pair OYD123/OYD045. The two PCR products were used as template for overlap extension PCR with primer pair OYD122/OYD123. The amplified fragment was cut with BamHI and EcoRI and cloned into pminiMAD cut with the same enzymes.

pYD131 was generated with overlap extension PCR. The "UP" product was amplified from *Bs*168 genomic DNA with primer pair OYD362/OYD390. The "DOWN" product was amplified from *Bs168* genomic DNA with primer pair OYD363/OYD389. The two PCR products were used as template for overlap extension PCR with primer pair OYD362/OYD363. The amplified fragment was cut with HindIII and NheI and cloned into pDR111 cut with the same enzymes.

pYD132 was generated by cloning the PCR product from OYD006 and OYD526 amplification of *Bs*168 genomic DNA into pDR111 (BamHI-SphI).

pYD133 was generated by cloning the PCR product from OYD362 and OYD384 amplification of *Bs*168 genomic DNA into pDR111 (HindII-NheI).

pYD134 was generated with overlap extension PCR. The "UP" product was amplified from *Bs*168 genomic DNA with primer pair OYD362/OYD394. The "DOWN" product was amplified from *Bs168* genomic DNA with primer pair OYD363/OYD393. The two PCR products were used as template for overlap extension PCR with primer pair OYD362/OYD363. The amplified fragment was cut with HindIII and NheI and cloned into pDR111 cut with the same enzymes.

pYD135 was generated with overlap extension PCR. The "UP" product was amplified from *Bs*168 genomic DNA with primer pair OYD362/OYD306. The "DOWN" product was amplified from *Bs168* genomic DNA with primer pair OYD305/OYD363. The two PCR products were used as template for overlap extension PCR with primer pair OYD006/OYD302. This PCR product was used as template for PCR with primer pair OYD362/OYD363. The amplified fragment was cut with HindIII and NheI and cloned into pDR111 cut with the same enzymes.

pYD136 was generated with overlap extension PCR. The "UP" product was amplified from *Bs*168 genomic DNA with primer pair OYD362/OYD396. The "DOWN" product was amplified from *Bs168* genomic DNA with primer pair OYD363/OYD395. The two PCR products were used as template for overlap extension PCR with primer pair OYD362/OYD363. The amplified fragment was cut with HindIII and NheI and cloned into pDR111 cut with the same enzymes.

pYD137 was generated with overlap extension PCR. The "UP" product was amplified from *Bs*168 genomic DNA with primer pair OYD368/OYD392. The "DOWN" product was amplified from *Bs168* genomic DNA with primer pair OYD369/OYD391. The two PCR products were used as template for overlap extension PCR with primer pair OYD368/OYD369. The amplified fragment was cut with BamHI and EcoRI and cloned into pminiMAD cut with the same enzymes.

pYD138 was generated with overlap extension PCR. The "UP" product was amplified from *Bs*168 genomic DNA with primer pair OYD368/OYD400. The "DOWN" product was amplified from *Bs168* genomic DNA with primer pair OYD369/OYD399. The two PCR products were used as template for overlap extension PCR with primer pair OYD368/OYD369. The amplified fragment was cut with BamHI and EcoRI and cloned into pminiMAD cut with the same enzymes.

pYD139 was generated with overlap extension PCR. The "UP" product was amplified from *Bs*168 genomic DNA with primer pair OYD006/OYD400. The "DOWN" product was amplified from *Bs168* genomic DNA with primer pair OYD369/ OYD399. The two PCR products were used as template for overlap extension PCR with primer pair OYD006/OYD369. This PCR product was used as template for PCR with primer pair OYD006/OYD007. The amplified fragment was cut with BamHI and SphI and cloned into pCH363 cut with the same enzymes.

pYD140 was generated by cloning PCR product from OYD362 and OYD363 amplification of pYD139 into pDR111 (HindII-NheI).

pYD141 was generated with overlap extension PCR. The "UP" product was amplified from *Bs*168 genomic DNA with primer pair OYD362/OYD402. The "DOWN" product was amplified from *Bs168* genomic DNA with primer pair OYD369/ OYD401. The two PCR products were used as template for overlap extension PCR with primer pair OYD362/OYD369. This PCR product was used as template for PCR with primer pair OYD362/OYD363. The amplified fragment was cut with HindIII and NheI and cloned into pDR111 cut with the same enzymes.

pYD142 was generated with overlap extension PCR. The "UP" product was amplified from *Bs*168 genomic DNA with primer pair OYD362/OYD404. The "DOWN" product was amplified from *Bs168* genomic DNA with primer pair OYD369/ OYD403. The two PCR products were used as template for overlap extension PCR with primer pair OYD362/OYD369. This PCR product was used as template for PCR with primer pair OYD362/OYD363. The amplified fragment was cut with HindIII and NheI and cloned into pDR111 cut with the same enzymes.

pYD143 was generated with overlap extension PCR. The "UP" product was amplified from *Bs*168 genomic DNA with primer pair OYD362/OYD406. The "DOWN" product was amplified from *Bs168* genomic DNA with primer pair

OYD363/ OYD405. This PCR product was used as template for PCR with primer pair OYD362/OYD363. The amplified fragment was cut with HindIII and NheI and cloned into pDR111 cut with the same enzymes.

pYD146 was generated by cloning the PCR product from OYD006 and OYD007 amplification of pYD135 into pCH363 (SphI-BamHI).

pYD165 was generated with overlap extension PCR. The "UP" product was amplified from *Bs*168 genomic DNA with primer pair OYD215/OYD306. The "DOWN" product was amplified from *Bs168* genomic DNA with primer pair OYD216/OYD305. The two PCR products were used as template for overlap extension PCR with primer pair OYD215/OYD216. The amplified fragment was cut with BamHI and EcoRI and cloned into pminiMAD cut with the same enzymes.

pYD166 was generated with overlap extension PCR. The "UP" product was amplified from *Bs*168 genomic DNA with primer pair OYD215/OYD498. The "DOWN" product was amplified from *Bs168* genomic DNA with primer pair OYD216/OYD491. The two PCR products were used as template for overlap extension PCR with primer pair OYD215/OYD216. The amplified fragment was cut with BamHI and EcoRI and cloned into pminiMAD cut with the same enzymes.

pYD167 was generated with overlap extension PCR. The "UP" product was amplified from *Bs*168 genomic DNA with primer pair OYD215/OYD493. The "DOWN" product was amplified from *Bs168* genomic DNA with primer pair OYD216/OYD492. The two PCR products were used as template for overlap extension PCR with primer pair OYD215/OYD216. The amplified fragment was cut with BamHI and EcoRI and cloned into pminiMAD cut with the same enzymes.

pYD168 was generated with overlap extension PCR. The "UP" product was amplified from *Bs*168 genomic DNA with primer pair OYD215/OYD495. The "DOWN" product was amplified from *Bs168* genomic DNA with primer pair OYD216/OYD494. The two PCR products were used as template for overlap extension PCR with primer pair OYD215/OYD216. The amplified fragment was cut with BamHI and EcoRI and cloned into pminiMAD cut with the same enzymes.

pYD169 was generated with overlap extension PCR. The "UP" product was amplified from *Bs*168 genomic DNA with primer pair OYD215/OYD497. The "DOWN" product was amplified from *Bs168* genomic DNA with primer pair OYD216/OYD496. The two PCR products were used as template for overlap extension PCR with primer pair OYD215/OYD216. The amplified fragment was cut with BamHI and EcoRI and cloned into pminiMAD cut with the same enzymes.

pYD170 was generated with overlap extension PCR. The "UP" product was amplified from *Bs*168 genomic DNA with primer pair OYD362/OYD398. The "DOWN" product was amplified from *Bs168* genomic DNA with primer pair OYD369/ OYD397. The two PCR products were used as template for overlap extension PCR with primer pair OYD362/OYD369. This PCR product was used as template for PCR with primer pair OYD362/OYD363. The amplified fragment was cut with HindIII and NheI and cloned into pDR111 cut with the same enzymes.

pYD171 was generated by cloning the PCR product from OYD362 and OYD363 amplification of pYD129 into pDR111 (HindII-NheI).

pYD172 was generated by cloning the PCR product from OYD362 and OYD363 amplification of pYD101 into pDR111 (HindII-NheI).

pYD173 was generated by cloning the PCR product from OYD006 and OYD007 amplification of pYD166 into pCH363 (SphI-BamHI).

pYD174 was generated by cloning the PCR product from OYD006 and OYD007 amplification of pYD167 into pCH363 (SphI-BamHI).

pYD175 was generated by cloning the PCR product from OYD006 and OYD007 amplification of pYD168 into pCH363 (SphI-BamHI).

pYD176 was generated by cloning the PCR product from OYD006 and OYD007 amplification of pYD169 into pCH363 (SphI-BamHI).

pYD177 was generated by cloning the PCR product from OYD006 and OYD007 amplification of pYD125 into pCH363 (SphI-BamHI).

pYD178 was generated with overlap extension PCR. The "UP" product was amplified from *Bs*168 genomic DNA with primer pair OYD122/OYD311. The "DOWN" product was amplified from *Bs168* genomic DNA with primer pair OYD310/OYD011. The two PCR products were used as template for overlap extension PCR with primer pair OYD122/OYD011. This PCR product was used as template for PCR with primer pair OYD035/OYD011. The amplified fragment was cut with BamHI and KpnI and cloned into pKNT25 cut with the same enzymes.

pYD179 was generated with overlap extension PCR. The "UP" product was amplified from *Bs*168 genomic DNA with primer pair OYD122/OYD313. The "DOWN" product was amplified from *Bs168* genomic DNA with primer pair OYD312/OYD011. The two PCR products were used as template for overlap extension PCR with primer pair OYD122/OYD011. This PCR product was used as template for PCR with primer pair OYD035/OYD011. The amplified fragment was cut with BamHI and KpnI and cloned into pKNT25 cut with the same enzymes.

pYD180 was generated with overlap extension PCR. The "UP" product was amplified from *Bs*168 genomic DNA with primer pair OYD122/OYD315. The "DOWN" product was amplified from *Bs168* genomic DNA with primer pair OYD314/OYD011. The two PCR products were used as template for overlap extension PCR with primer pair OYD122/OYD011. This PCR product was used as template for PCR with primer pair OYD035/OYD011. The amplified fragment was cut with BamHI and KpnI and cloned into pKNT25 cut with the same enzymes.

pYD181 was generated with overlap extension PCR. The "UP" product was amplified from *Bs*168 genomic DNA with primer pair OYD122/OYD317. The "DOWN" product was amplified from *Bs168* genomic DNA with primer pair OYD316/OYD011. The two PCR products were used as template for overlap extension PCR with primer pair OYD122/OYD011. This PCR product was used as template for PCR with primer pair OYD035/OYD011. The amplified fragment was cut with BamHI and KpnI and cloned into pKNT25 cut with the same enzymes.

pYD182 was generated with overlap extension PCR. The "UP" product was amplified from *Bs*168 genomic DNA with primer pair OYD035/OYD528. The "DOWN" product was amplified from *Bs168* genomic DNA with primer pair OYD527/OYD011. The two PCR products were used as template for overlap extension PCR with primer pair OYD035/OYD011. The amplified fragment was cut with BamHI and KpnI and cloned into pKNT25 cut with the same enzymes.

pYD183 was generated with overlap extension PCR. The "UP" product was amplified from *Bs*168 genomic DNA with primer pair OYD035/OYD331. The "DOWN" product was amplified from *Bs168* genomic DNA with primer pair OYD330/OYD011. The two PCR products were used as template for overlap extension PCR with primer pair OYD035/OYD011. The amplified fragment was cut with BamHI and KpnI and cloned into pKNT25 cut with the same enzymes.

pYD184 was generated with overlap extension PCR. The "UP" product was amplified from *Bs*168 genomic DNA with primer pair OYD035/OYD327. The "DOWN" product was amplified from *Bs168* genomic DNA with primer pair OYD326/OYD011. The two PCR products were used as template for overlap extension PCR with primer pair OYD035/OYD011. The amplified fragment was cut with BamHI and KpnI and cloned into pKNT25 cut with the same enzymes.

pYD185 was generated with overlap extension PCR. The "UP" product was amplified from *Bs*168 genomic DNA with primer pair OYD035/OYD518. The "DOWN" product was amplified from *Bs168* genomic DNA with primer pair OYD517/OYD011. The two PCR products were used as template for overlap extension PCR with primer pair OYD035/OYD011. The amplified fragment was cut with BamHI and KpnI and cloned into pKNT25 cut with the same enzymes.

pYD186 was generated with overlap extension PCR. The "UP" product was amplified from *Bs*168 genomic DNA with primer pair OYD035/OYD329. The "DOWN" product was amplified from *Bs168* genomic DNA with primer pair OYD328/OYD011. The two PCR products were used as template for overlap extension PCR with primer pair OYD035/OYD011. The amplified fragment was cut with BamHI and KpnI and cloned into pKNT25 cut with the same enzymes.

pYD187 was generated by cloning the PCR product from OYD006 and OYD007 amplification of pYD129 into pCH363 (SphI-BamHI).

REFERENCES

Cho, E., N. Ogasawara & S. Ishikawa, (2008) The functional analysis of YabA, which interacts with DnaA and regulates initiation of chromosome replication in Bacillus subtils. *Genes & genetic systems* **83**: 111-125.

Jameson, K.H., N. Rostami, M.J. Fogg, J.P. Turkenburg, A. Grahl, H. Murray & A.J. Wilkinson, (2014) Structure and interactions of the *Bacillus subtilis* sporulation inhibitor of DNA replication, SirA, with domain I of DnaA. *Mol Microbiol* **93**: 975-991.

Kearns, D.B. & R. Losick, (2005) Cell population heterogeneity during growth of Bacillus subtilis. *Genes & development* **19**: 3083-3094.

Ozaki, S., H. Kawakami, K. Nakamura, N. Fujikawa, W. Kagawa, S.Y. Park, S. Yokoyama, H. Kurumizaka & T. Katayama, (2008) A common mechanism for the ATP-DnaA-dependent formation of open complexes at the replication origin. *J Biol Chem* **283**: 8351-8362.

Scholefield, G., J. Errington & H. Murray, (2012) Soj/ParA stalls DNA replication by inhibiting helix formation of the initiator protein DnaA. *The EMBO journal* **31**: 1542-1555.

Scholefield, G. & H. Murray, (2013) YabA and DnaD inhibit helix assembly of the DNA replication initiation protein DnaA. *Mol Microbiol* **90**: 147-159.

Youngman, P.J., J.B. Perkins & R. Losick, (1983) Genetic transposition and insertional mutagenesis in Bacillus subtilis with Streptococcus faecalis transposon Tn917. *Proceedings of the National Academy of Sciences of the United States of America* **80**: 2305-2309.

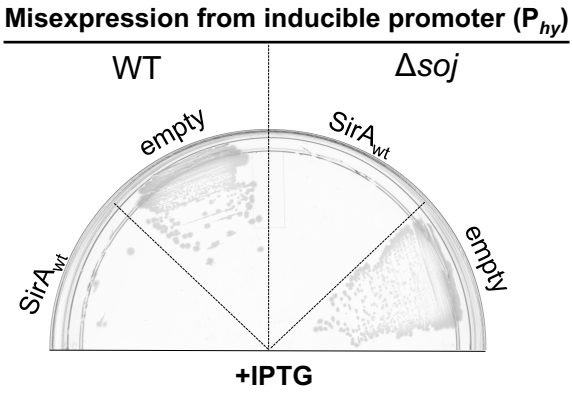
Misexpression from inducible promoter (P_{hy})
WT
Δ*soj*
empty
$SirA_{wt}$
$SirA_{wt}$
empty
+IPTG

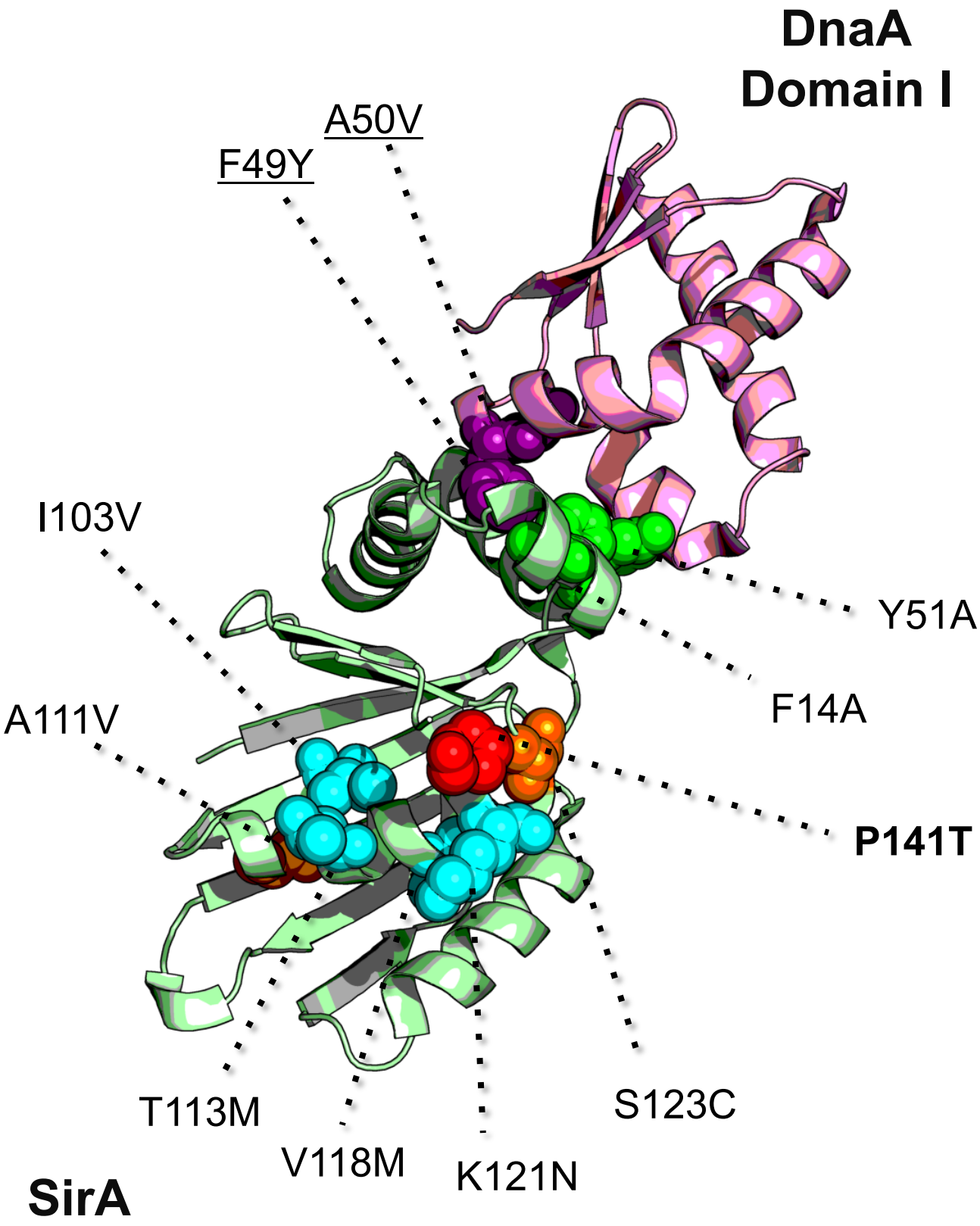
DnaA
Domain I
A50V
F49Y
I103V
Y51A
F14A
A111V
P141T
T113M
V118M
K121N
S123C
SirA

Misexpression of $SirA_{S123C}$ from inducible promoter (P_{hy})

CH/37°C/ 1 mM IPTG

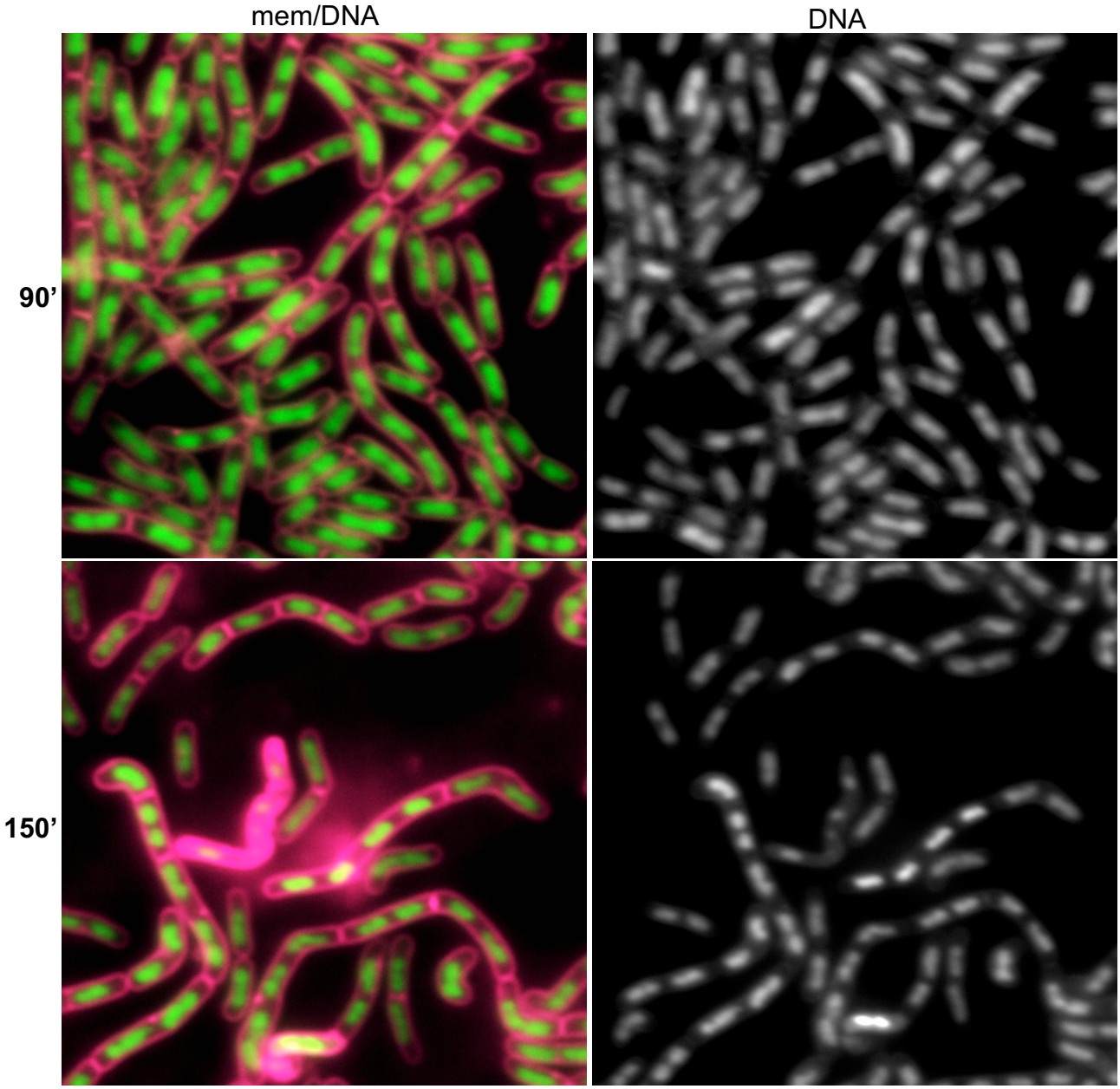

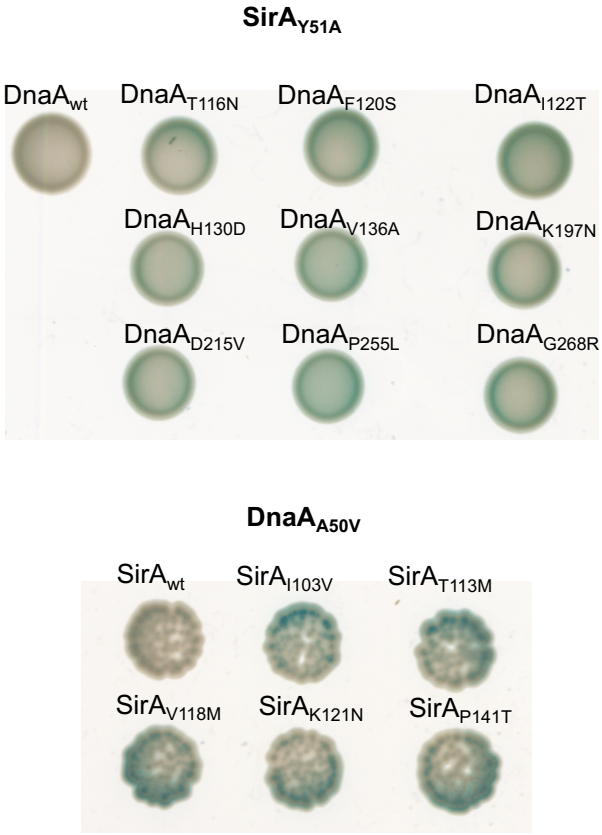
SirA$_{Y51A}$
DnaA$_{wt}$
DnaA$_{T116N}$
DnaA$_{F120S}$
DnaA$_{I122T}$
DnaA$_{H130D}$
DnaA$_{V136A}$
DnaA$_{K197N}$
DnaA$_{D215V}$
DnaA$_{P255L}$
DnaA$_{G268R}$
DnaA$_{A50V}$
SirA$_{wt}$
SirA$_{I103V}$
SirA$_{T113M}$
SirA$_{V118M}$
SirA$_{K121N}$
SirA$_{P141T}$

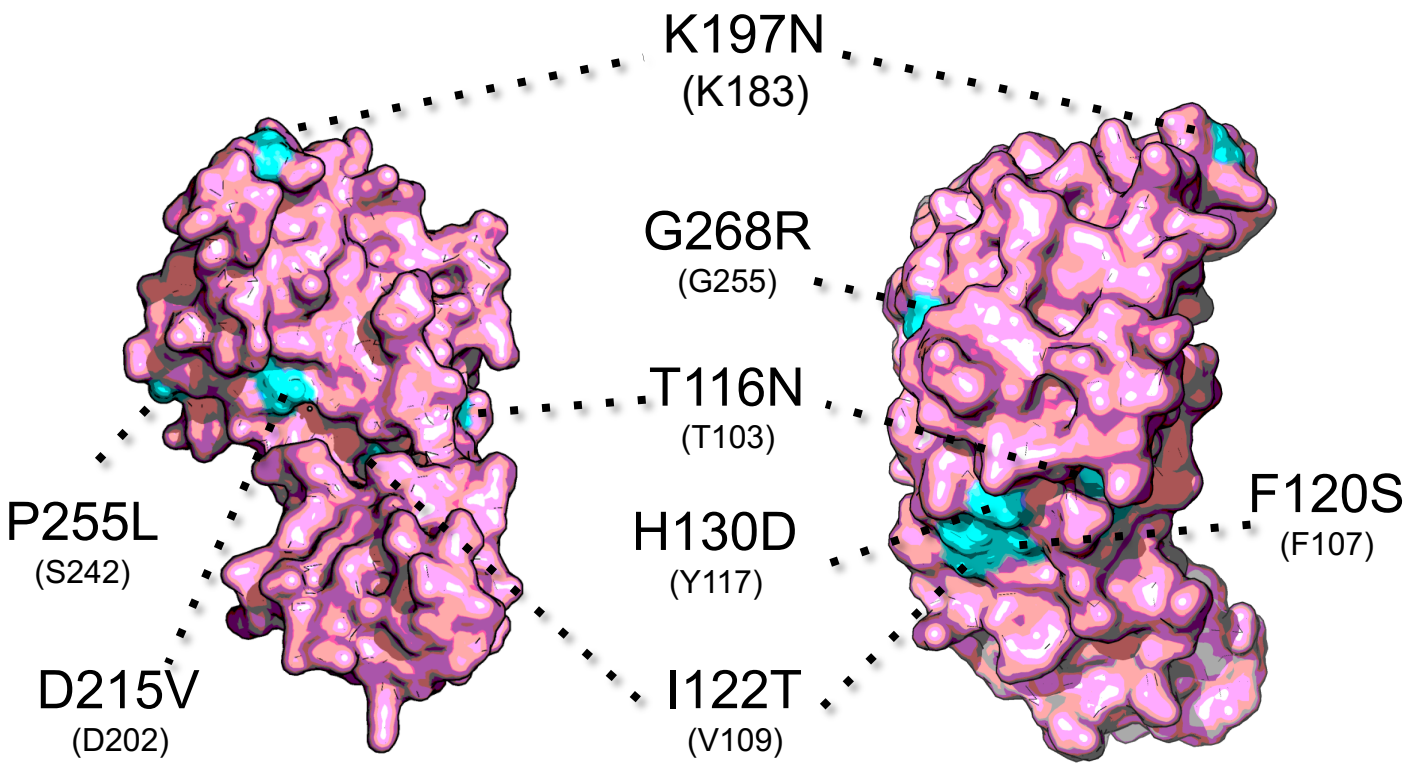


```
T. maritima DnaA     1 ------MKERILQEIKTRVNRKSWELWFSSFDVKSIEGNKVVFSVGNLFIKEWLEKKYYS
B. subtilis DnaA     1 MENILDLWNQALAQIEKKLSKPSFETWMKSTKAHSLQGDTLTITAPNEFARDWLESRYLH
    E. coli DnaA     1 --MSLSLWQQCLARLQDELPATEFSMWIR-PLQAELSDNTLALYAPNRFVLDWVRDKYLN

T. maritima DnaA    55 VLSKAVKVVLGNDA-----------------------------TFEITYEAFEPHSSY
B. subtilis DnaA    61 LIADTIYELTGEELSIKFVIP-----------------------QNQDVEDFMPKPQVK
    E. coli DnaA    58 NINGLLTSFCGADAPQLRFEVGTKPVTQTPQAAVTSNVAAPAQVAQTQPQRAAPSTRSGW

T. maritima DnaA    84 SEPLVKKRAVLLTPLNPDYTFENFVVGPGNSFAYHAALEVAKHPG-RYNPLFIYGGVGLG
B. subtilis DnaA    97 KAVKEDTSDFPQNMLNPKYTFDTFVIGSGNRFAHAASLAVAEAPAKAYNPLFIYGGVGLG
    E. coli DnaA   118 DNVPAPAEPTYRSNVNVKHTFDNFVEGKSNQLARAAARQVADNPGGAYNPLFLYGGTGLG

T. maritima DnaA   143 KTHLLQSIGNYVVQNEPDLRVMYITSEKFLNDLVDSMKEGKLNEFREKYRKKVDILLIDD
B. subtilis DnaA   157 KTHLMHAIGHYVIDHNPSAKVVYLSSEKFTNEFINSIRDNKAVDFRNRYRN-VDVLLIDD
    E. coli DnaA   178 KTHLLHAVGNGIMARKPNAKVVYMHSERFVQDMVKALQNNAIEEFKRYYRS-VDALLIDD

T. maritima DnaA   203 VQFLIGKTGVQTELFHTFNELHDSGKQIVICSDREPQKLSEFQDRLVSRFQMGLVAKLEP
B. subtilis DnaA   216 IQFLAGKEQTQEEFFHTFNTLHEESKQIVISSDRPPKEIPTLEDRLRSRFEWGLITDITP
    E. coli DnaA   237 IQFFANKERSQEEFFHTFNALLEGNQQIILTSDRYPKEINGVEDRLKSRFGWGLTVAIEP

T. maritima DnaA   263 PDEETRKSIARKMLEIEHGELPEEVLNFVAENVDDNLRRLRGAIIKLLVYKETTGKEVDL
B. subtilis DnaA   276 PDLETRIAILRKKAKAEGLDIPNEVMLYIANQIDSNIRELEGALIRVVAYSSLINKDINA
    E. coli DnaA   297 PELETRVAILMKKADENDIRLPGEVAFFIAKRLRSNVRELEGALNRVIANANFTGRAITI

T. maritima DnaA   323 KEAILLLKDFIKPNRVKAMDPIDELIEIVAKVTGVPREEILSNSRNVKALTARRIGMYVA
B. subtilis DnaA   336 DLAAEALKDIIPSSKPKVIT-IKEIQRVVGQQFNIKLEDFKAKKRTKSVAFPRQIAMYLS
    E. coli DnaA   357 DFVREALRDLLALQ-EKLVT-IDNIQKTVAEYYKIKVADLLSKRRSRSVARPRQMAMALA

T. maritima DnaA   383 KNYLKSSLRTIAEKFNRSHPVVVDSVKKVKDSLLKGNKQLKALIDEVIGEISRRALSG
B. subtilis DnaA   395 REMTDSSLPKIGEEFGGRDHTTVIHAHEKISKLLADDEQLQQHVKEIKEQLK------
    E. coli DnaA   415 KELTNHSLPEIGDAFGGRDHTTVLHACRKIEQLREESHDIKEDFSNLIRTLSS------
```